QUANTIFYING MECHANORECEPTORS IN A PORCINE ACL: A COMPARATIVE ANALYSIS OF HISTOLOGICAL STAINING METHODS

By

AMULYA KADABA

B.S, TEXAS A&M UNIVERSITY, 2023

Thesis

Submitted in partial fulfillment of the requirements for the Degree of Master of Science in the Graduate Program of Biomedical Engineering at Brown University

PROVIDENCE, RHODE ISLAND

MAY 2025

AUTHORIZATION TO LEND AND REPRODUCE THE THESIS

As the sole author of this thesis, I authorize Brown University to lend it to other institutions for the purpose of scholarly research.

Date_____ _____

AMULYA KADABA, Author

I further authorize Brown University to reproduce this thesis by photocopying or other means, in total or in part, at the request of other institutions or individuals for the purpose of scholarly research.

Date_____ _____

AMULYA KADABA, Author

This thesis by Amulya Kadaba is accepted in its present form by the Center of Biomedical Engineering as satisfying the thesis requirements for the degree of Master of Science

Date_____ Signature: _____

Dr. Braden Fleming, Advisor

Date_____ Signature: _____

Dr. Jillian E. Beveridge, Reader

Date_____ Signature: _____

Dr. Vikas Srivastava, Reader

Approved by the Graduate Council

Date_____ Signature: _____

Dr. Marissa Gray, Biomedical Engineering Master's Program Director

Acknowledgements

Over the past two years, this project has been at the center of my academic and personal journey, and I am deeply grateful to everyone who has helped me reach the finish line. My time at Brown has been filled with moments of challenge and growth, and I've been fortunate to meet incredible individuals whose support has meant the world to me.

First and foremost, I would like to thank those who have guided and supported me academically. I am especially grateful to my faculty advisor, Dr. Braden Fleming, for giving me the opportunity to work on this project and for providing me with the resources, trust, and mentorship needed to succeed. I would also like to sincerely thank my committee members, Dr. Jillian Beveridge and Dr. Vikas Srivastava, whose thoughtful feedback and guidance helped me refine my thesis and push it to a higher standard. A special thank you goes to Anika Breker, who played a critical role in the data analysis as the second examiner of my thesis. Her involvement was vital in achieving the repeatability aspect of this study, fulfilling the third objective of my work. I also owe much gratitude to Peter Caradonna at the University of New England, whose expertise was invaluable in optimizing the NFP staining protocol and capturing the histological images of the porcine ligaments.

To everyone at Brown University who supported me, thank you for being part of this journey!

Beyond academics, I am incredibly grateful to those who stood by me through the highs and lows of this rollercoaster experience. To my parents, Uma Kadaba and Kadaba Srinivasamurthy, your unconditional love and unwavering belief in me have been my greatest strength. You both have always been my inspiration, and I dedicate this thesis, and all that I have accomplished, to you both.

To my sister, Dr. Aishwarya Murthy, you've been my role model and constant source of encouragement. Your example has taught me that success is built not only through hard work but also through kindness and character. Thank you for being my rock since day one.

To my friends, thank you for listening to my daily rants and celebrating the small wins with me. Your presence and support made even the toughest days easier.

And finally, to someone very close to my heart, Gaurav. Thank you for your patience, love, and unwavering encouragement. Your belief in me kept me going, even when I doubted myself.

Funding

This study was funded by the Lucy Lippitt endowment of the Department of Orthopaedics at the Warren Alpert Medical School of Brown University. The histology was optimized and performed by Center of Biomedical Research Excellence (COBRE) Histology and Imaging Core at the University of New England (NIGMS P20-GM103643) under the direction of the Core manager, Peter Caradonna.

Table of Contents

List of Figures

Abstract

Anterior cruciate ligament (ACL) injuries account for nearly 50% of all knee injuries, with over 200,000 cases annually in the United States. Centrally located in the knee joint, the ACL contributes to sensorimotor regulation through embedded mechanoreceptors that facilitate proprioception and maintain joint stability via ligament-induced neuromuscular reflexes. Damage to the ACL disrupts these pathways, increasing the risk of re-injury. Establishing a baseline quantification of mechanoreceptors in healthy, native ACLs is therefore essential to assess neural restoration following surgical interventions. One such intervention, the Bridge-Enhanced ACL Repair (BEAR) technique, promotes intrinsic healing rather than relying on graft replacement. Because BEAR preserves native tissue, it is hypothesized to better retain or support the regeneration of mechanoreceptors, potentially restoring proprioceptive function more effectively than traditional methods.

This study aimed to characterize the total number and spatial distribution of mechanoreceptors in healthy, native porcine ACLs. Mechanoreceptor presence was mapped along the insertion-ligament-insertion axis and across the ligament's transverse width through its sagittal slices to establish a foundational reference for future comparisons with reconstructed and BEAR-repaired tissues. Additionally, an optimized histological staining protocol was developed to enhance visualization and quantification. A total of 429 mechanoreceptors were identified by Examiner 1 and 539 by Examiner 2, with an inter-examiner overlap of 88.6%. These counts exceed those reported in earlier studies, likely due to improved staining techniques and detailed evaluation protocols. Mechanoreceptors were most densely concentrated at the ligament's insertion sites but were also observed in the mid-substance. This spatial pattern aligns with trends reported in existing literature, reinforcing the biological relevance of the findings. Across

the transverse width, a distinct pattern of increasing mechanoreceptor presence from the center toward one end was observed.

Overall, this study contributes key anatomical and methodological insights to the field of ligament neurobiology. It provides an optimized approach for mechanoreceptor staining and quantification and establishes a critical reference point for evaluating proprioceptive restoration in ACL repair, particularly for biologically driven approaches like BEAR.

Chapter 1: Introduction

Functionality of Ligaments

The knee joint is composed of three bones: the femur, tibia, and patella. It is stabilized by four primary ligaments: the anterior cruciate ligament (ACL), posterior cruciate ligament (PCL), medial collateral ligament (MCL), and lateral collateral ligament (LCL). These ligaments function to hold the bones together, provide joint stability, and guide the knee through its normal range of motion [1, 2]. Structurally, ligaments are composed of dense collagenous fibers anchored to the bone at both ends[1, 3]. Although they may appear as singular structures, ligaments are organized hierarchically into groups of parallel fibers[1] . Depending on bone positioning and applied forces, individual fibers within the ligament tighten or loosen [1].

Importance of ACL

Anterior cruciate ligament (ACL) disruption is one of the most common knee injuries, accounting for approximately 50% of all knee injuries, with over 200,000 ACL tears occurring annually in the United States [4, 5]. Located at the center of the knee, the ACL functions to constrain anterior translation of the tibia while guiding knee flexion-extension and axial rotation [6]. Additionally, it plays a role in regulating excitatory and inhibitory control of the surrounding musculature [7]. ACL injuries typically result from sudden twisting motions [8] or impact forces, such as landing from a jump [9]. Damage to the ACL disrupts neural receptors, impairing sensorimotor control [10]. When the ligament is compromised, the somatosensory system is unable to accurately convey positional and movement-related information about the joint and body [10], leading to altered neuromuscular control even during simple flexion tasks [11].

Mechanoreceptors and Their Role:

Proprioceptive stimuli from somatosensory receptors in the ligaments detect the position, movement, or acceleration of a body part based on the internal forces on the body [12-14]. This information is transmitted through mechanoreceptors, a type of somatosensory receptor, that can detect external stimuli, such as touch, pressure, stretching, and motion, and relays them to the central nervous system [15]. The central nervous system then receives, processes, and responds to this information [16]. Even without visual cues, an individual can react to external stimuli and positional changes in their muscles, tendons, or joints due to the neural structures that transmit

information to the central nervous system [12]. Additionally, proprioception regulates muscle activity and reflex responses to mechanical deformation of the ligament [14], highlighting the critical role of neural structures within the ligament.

Functionality of mechanoreceptors

The primary neurosensory receptors in the ACL include Golgi tendon organs, Ruffini endings (also referred to as Ruffini corpuscles in some literature), Pacinian corpuscles, and free nerve endings [17-19]. These receptors help protect the knee joint from injury by mediating ligament-induced neuromuscular reflexes [20]. In this reflex pathway, mechanoreceptors detect mechanical changes within the ligament and send afferent signals to the central nervous system, which processes the information and then generates efferent signals to activate or relax specific muscles in response [21]. A well-known example of this is the ACL–hamstring reflex arc, where sufficient stimulation of the ACL triggers a reflexive activation of the hamstring muscles to help stabilize the joint [21].

Each mechanoreceptor type contributes differently to this neuromuscular control. The Golgi tendon organs detect tension within the ligament and send inhibitory signals to reflexively relax the necessary muscles under excessive strain [22-24]. Ruffini endings respond to ligament elongation by detecting collagen fiber deformation [12, 14, 25]. While both Ruffini endings and Golgi tendon organs contribute to neuromuscular control, the Golgi tendon organ has a higher activation threshold and primarily functions during extreme joint stress, whereas Ruffini endings help maintain baseline muscle tone [14, 18, 26]. Pacinian corpuscles, on the other hand, detect vibration and deep pressure [27]. Unlike these pressure-sensitive receptors, free nerve endings function as nociceptors that detect pain [18].

Known characteristics of mechanoreceptors

Studies have shown that mechanoreceptors are primarily concentrated at the tibial and femoral insertions of the ACL [18, 19]. A review by Hogervorst et al. examined mechanoreceptor morphology and size, referencing Freeman and Wyke's classification system [26], which has been widely used for identifying and categorizing mechanoreceptors [28]. While the presence of mechanoreceptors in the ACL has been evaluated [4, 17, 29-31], there still is no consensus on their precise identity and quantity [31-33]. Han et al. identified the four primary

mechanoreceptors in addition to “atypical” mechanoreceptors within the ACL [19], with atypical mechanoreceptors being the third most common nerve ending. Atypical mechanoreceptors were classified as those that had irregular morphology, disordered structure and were of various sizes [19]. This raises the question of whether these structures represent an unclassified mechanoreceptor distinct from the established four types or just due to the orientation of the receptor relative to the sectioning plane.

A review by Banios et al. examined studies quantifying mechanoreceptors in healthy ACLs, identifying a total of 19 mechanoreceptors across two normal ACLs near both ligament insertions, including eight Ruffini corpuscles and eleven Golgi tendon organs [14]. Georgoulis et al. used a modified gold chloride staining technique to observe Ruffini, Pacinian, and Golgi-like mechanoreceptors in ACL remnants of patients with torn ACLs [34]. Similarly, Sha et al. identified approximately twelve Ruffini-like corpuscles and one Pacinian-like corpuscle in the healthy ACLs of six individuals [35]. Adachi et al. found a positive correlation between mechanoreceptor quantity in an injured ACL and proprioceptive knee function, as assessed through joint position sense testing before ACL reconstruction surgery [36]. This result suggests that establishing a baseline quantification of mechanoreceptors in native ligaments is crucial for evaluating ACL healing or graft function post-surgery.

Further evidence from Dhillon et al. supports the role of mechanoreceptors in proprioception restoration, as normal mechanoreceptors were identified in 46% of ACL remnant stumps across 63 patients with ACL injuries [31]. Additionally, a significant correlation was observed between the time since injury and mechanoreceptor quantity [31]. These findings suggest that timely surgical intervention could enhance proprioceptive recovery in ACL injuries. However, due to variations in staining techniques and inconsistencies in reported findings, the results across studies are inconsistent. Further research is necessary to comprehensively and accurately characterize mechanoreceptors in a normal ACL and their role in knee neuromuscular control to serve as baseline measures.

Implications for ACL Reconstruction and BEAR Technique

Establishing a baseline quantification of mechanoreceptors in healthy native ligaments is crucial for evaluating ACL or graft healing post-surgery to determine if the neural structures are preserved or restored following ACL surgery. ACL reconstruction is a surgical procedure in

which the damaged ligament is removed and replaced with a tendon graft [37]. During this process, all neural elements of the ACL are severed and removed [7]. Several studies have examined neural structure regeneration in healing grafts after ACL reconstruction [5, 7, 32, 38, 39]. Notably, Young et al. found no significant differences in neurofilament protein (NFP) concentration, a marker of axon cylinders carrying proprioceptive fibers, between allografts (cadaveric grafts) and autografts (patient-derived grafts), but both exhibited a lower concentration compared to native ACL tissue [5].

Additionally, mechanoreceptors in ACL grafts appear to be absent or diminished over time. Kim et al. observed that mechanoreceptors in ACL allografts did not regenerate with time, with no detectable presence of mechanoreceptors within the allograft even 26 months after surgery [39]. Similarly, Krogsgaard et al. assessed leg muscular reflexes to determine the functionality of mechanoreceptors and their impact on neuromuscular control [7]. Electrical stimulation of reflex pathways in reconstructed ACLs required 3.4 times the stimulation of a normal ligament, indicating a failure of reinnervation post-surgery [7]. Nyland et al. proposed that the only viable method to preserve mechanoreceptor function is ACL repair, rather than reconstruction, as this should preserve the integrity of neural structures necessary for proprioceptive recovery [20].

The Bridge-Enhanced ACL Repair (BEAR) technique offers a promising alternative to conventional ACL reconstruction by facilitating biological healing of the ligament rather than replacing it with a graft [40]. This method integrates primary suture repair with a specialized extracellular matrix scaffold (the BEAR scaffold; Miach Orthopaedics LLC), which is placed between the two torn ends of the ACL and activated using the patient's blood [40]. The scaffold serves as a bridge, allowing the ligament to heal without requiring direct re-approximation of the torn ends [40]. In a two-year follow-up study, Murray et al. reported that BEAR yielded comparable outcomes to ACL reconstruction and quicker restoration of muscle function [40]. Given that BEAR may preserve native ACL structures, it is hypothesized that mechanoreceptor retention and growth may be superior to that observed in ACL reconstructions.

Histological Evaluation of Mechanoreceptors

In reviewing the literature, it is clear there has been a lack of standardization in the histological methods used to determine the presence of mechanoreceptors in the ACL, leading to

a high rate of uncertainty and discrepancy between studies [33, 41]. Various histological techniques have been employed, yet the optimal staining approach remains unclear. This study aims to identify and optimize the most effective staining technique for porcine ACL histology, including immunohistochemical (IHC) methods and metallic salts such as gold chloride and silver staining. Additionally, a preliminary analysis was conducted to quantify neural elements in the normal porcine ACL and compare findings between two independent examiners. The results of this study will serve as a foundation for future research evaluating mechanoreceptor differences among BEAR-treated, ACL-reconstructed, and healthy porcine ACLs.

Porcine Model

Along with addressing the lack of standardized staining protocols, careful consideration was given to selecting an appropriate animal model to ensure anatomical and biomechanical relevance for studying ACL mechanoreceptors. The porcine model was selected for this study due to its anatomical and biomechanical similarities to the human ACL [42-44]. Anatomically, porcine ACLs closely resemble human ACLs in terms of orientation, morphology, and attachment sites [42, 43]. Specifically, the femoral origins of the two ACL bundles in pigs follow the same pattern as those observed in humans, with a similar oblique orientation and characteristic hourglass-shaped morphology [42, 43].

Biomechanically, porcine ACLs mirror human ACL functionality by serving a comparable role in restricting anterior tibial translation and maintaining knee joint stability [42]. In cadaveric human knees, the ACL has been shown to provide approximately 86% of the total resisting force against anterior tibial translation, emphasizing its critical role in joint stabilization [42]. Additionally, the ultimate load to failure of the porcine ACL is similar to that of the human ACL [44], further supporting its suitability as a translational model for biomechanical and histological investigations. Given these parallels, the porcine model provides a highly relevant platform for studying mechanoreceptor distribution and neural structure restoration following ACL injury and repair. Following the selection of the porcine model, various histological techniques were evaluated to determine the most reliable histological technique for identifying mechanoreceptors.

S-100 Staining

Several studies have employed the S-100 antibody, an immunohistochemistry (IHC) technique, to stain a family of cytoplasmic calcium-binding proteins expressed in Schwann cells of the peripheral nervous system and in sensory neural structures such as mechanoreceptors [31, 45, 46]. With this technique, all types of mechanoreceptors in the ACL are directly stained [30, 45]. Rebmann et al. highlighted the reliability of the S-100 antibody to visualize and count the mechanoreceptors of the freshly ruptured ACL [45]. Of the seven studies that used the S-100 IHC technique, three successfully identified all four types of mechanoreceptors [19, 30, 31]. Among the other studies, three did not identify all of them [35, 45, 47], while the remaining study did not attempt to identify the type of mechanoreceptors [4]. A study by Chen et al. highlighted the necessity of using a combination of staining techniques, both S-100 and H&E (hematoxylin and eosin), to identify the four types of mechanoreceptors [48]. Pacinian corpuscles, which consist of multiple layers that are not nerve tissue, do not stain with S-100 alone [48]. To confirm their presence, H&E staining was used to visualize these layers, if present, the mechanoreceptor is classified as a Pacinian corpuscle, while the absence of layers suggests a Ruffini corpuscle [48]. Sha et al. identified Ruffini corpuscles, Pacinian corpuscles, and free nerve endings in the tibial remnants of ruptured ACLs [35]. Rebmann et al. only identified Ruffini corpuscles and free nerve endings in ACL grafts [45]. Chun et al. found Ruffini and Pacinian corpuscles in normal ACL remnants [47]. The protocol used by Chun et al. included fixing the tissue samples in formaldehyde, embedding them in paraffin, and cutting them into approximately 4-micron thick slices [47].

NFP Monoclonal Antibody

Neurofilament protein (NFP) antibody has been used to evaluate the presence of mechanoreceptors in ACL tissues [4, 5, 19, 31, 41, 49]. NFP stains nerve fibers and corpuscular endings [41, 50]. One published protocol details that the ACL tissue samples were frozen, cut into sections with a thickness of 6 micrometers, and fixed in acetone post-staining [51]. Unlike other techniques, the NFP antibody stains the neural structures by binding to the axons of mechanoreceptors associated with proprioception [4, 31]. Banios et al. highlighted that IHC techniques, such as NFP, have been frequently used due to their enhanced specificity compared to traditional histological methods (i.e., metallic salts) [14].

All four primary types of mechanoreceptors, including atypical mechanoreceptors in native ACLs, can be successfully stained with NFP, as demonstrated in the rabbit study by Han et al. [19]. This study estimated around 30 mechanoreceptors in a healthy rabbit ACL, including 13 Ruffini corpuscles, 4 Pacinian corpuscles, 3 Golgi tendon organs, and 9 atypical mechanoreceptors [19]. Lee et al. identified Ruffini corpuscles, Golgi corpuscles, and free nerve endings in the tibial remnant of ACLs [33]. Five studies used the NFP antibody to confirm the presence of normal mechanoreceptors through the ligament's immunoreactivity to the NFP antibody [4, 5, 31, 41, 49]. The NFP antibody has a significant positive correlation with the presence of morphologically normal mechanoreceptors in the remnants of ruptured ACLs [31, 41]. The NFP protocol provides good visual contrast for identifying mechanoreceptors and preventing misinterpretations [52]. Additionally, the NFP staining technique is advantageous as it can be performed on both frozen and fixed samples [51]. Thus, the NFP staining protocol is a reliable technique for determining the presence and quantification of the four primary mechanoreceptors, as well as any unclassified mechanoreceptors.

Polyclonal Antibody Against p75 and PGP 9.5

Two investigations used a combination of the p75 and PGP 9.5 immunohistochemistry (IHC) staining techniques in ACL remnants [35, 45], often performed alongside the S-100 IHC technique to confirm findings. P75 stains nerve growth factor, while PGP 9.5 is expressed in nerve tissues and serves as a marker for neuroendocrine cells [53, 54]. Rebmann et al. employed the p75 and PGP 9.5 antibodies to identify various mechanoreceptors in the torn ACL, using the S-100 technique to count the nerves, as S-100 has been shown to be a reliable marker [45]. Each technique stains different components of the neural structures, making their combined use advantageous [45].

Both studies were conducted using fixed human samples. Sha et al. evaluated torn ACL remnants, whereas Rebmann et al. assessed patellar tendon grafts following graft failure [35, 45]. Rebmann et al. identified Ruffini corpuscles and free endings in ACL grafts [45], while Sha et al. identified Ruffini endings, Pacinian corpuscles, and free endings in torn ACL remnants [35]. Tissue samples were fixed with a formalin solution, embedded in paraffin, and sectioned into 20-micrometer slices, with approximately 40 sections prepared per sample [35].

Gold chloride and Silver Staining

The earliest studies of the innervation of the ACL utilized either gold or silver staining [32, 55, 56]. These staining techniques heavily rely on the deposition or impregnation of the metallic salts in the tissue. Successful impregnation of the salts has been shown to be related to the ratio of the gold or silver solution to the thickness of the ligament sample [32, 38, 57]. The gold chloride solution stains the myelinated axons and sensory nerve endings, while the silver solution stains the axons [17, 32, 38]. Gold chloride and silver staining technique work with both frozen human and animal tissue samples [34, 38].

Many investigators have used various gold chloride staining methods, including the Bodian, Ranvier, O'Connor, Gairns, and Gonzales techniques, to identify the neural structures of ligaments, including the ACL [17, 34, 38, 39, 55, 56, 58]. Using gold chloride, Katonis et al and Schutte et al observed three of the four primary mechanoreceptors, Ruffini corpuscles, Pacinian corpuscles, and free nerve endings, in human cadaveric ACLs and posterior cruciate ligaments [56, 58]. In one study, free nerve endings made up 1 percent of the total area of the ruptured human ACL [49]. In a review article by Banios et al, it was reported that all four mechanoreceptors were present in the human ACL stump [14]. Similarly, Georgoulis et al successfully observed all four primary types of mechanoreceptors in the remnants of human ACLs [34]. The rabbit model also observed all four primary types of mechanoreceptors in reconstructed ACLs [38]. This study detailed their protocol and noted that tissue samples were frozen and sectioned at 100 μm thickness, with approximately 142 slices obtained per reconstructed ligament and 192 slices per control [38].

Review papers that compared the gold and silver staining techniques to immunohistochemical (IHC) methods, have demonstrated that IHC methods are easier to perform and more reliable in recognizing mechanoreceptors [14, 41, 52]. Witherspoon et al noted that the thickness of the sample, which varied between 25-100 μm, affected whether a mechanoreceptor was observed using gold chloride staining [57]. Therefore, sample thickness is critical for proper staining. In the study by Bali et al, it was reported that across multiple studies that used the gold chloride method, there was considerable variation in slice thickness, which contributed to a high variability in results [41]. They concluded that the gold chloride methods lacked standardization and that inconsistency in slice thickness could result in misinterpretation [33]. Goertzen et al observed that both gold chloride and silver staining failed to identify neural

structures in multiple stains over a 12-month period [32]. They reported that these techniques could only identify free nerve endings, which highlights the lack of reliability for the staining technique [32]. Thus, the primary disadvantages associated with gold and silver staining techniques are the sensitivity to sample thickness and their poor visual contrast resulting in a higher risk of misinterpreting results [33, 34, 36, 52]. Although this method has been used in many investigations, its lack of reliability and low visual contrast does not make it an ideal histology method.

Selected Techniques for Optimization

An effective histological technique for identifying neural structures within the anterior cruciate ligament (ACL) must be specific to mechanoreceptors, offer clear visual contrast, and remain cost-efficient. Among the available methods, immunohistochemical (IHC) staining using the neurofilament protein (NFP) antibody has emerged as the most reliable [14, 19, 31, 41, 52]. NFP staining has been consistently associated with the presence of functional mechanoreceptors, as it targets axon cylinders involved in proprioceptive signaling. In contrast, the S-100 antibody lacks specificity in distinguishing between mechanoreceptor subtypes such as Pacinian and Ruffini corpuscles. Specifically, the layered structure of Pacinian corpuscles cannot be effectively stained with S-100, thereby limiting the accuracy of mechanoreceptor classification. Although both S-100 and NFP staining techniques can provide strong visual contrast, NFP offers a higher degree of mechanoreceptor specificity. Alternative techniques, such as gold chloride or silver staining or the use of p75 and PGP 9.5 antibody combinations, have been reported to be less effective and incur higher costs. Given our long-term goal of evaluating differences in mechanoreceptors between normal ACLs, repaired ACLs, and ACL grafts using a porcine model, NFP antibodies were determined from this literature review to be the most suitable option. Furthermore, NFP has been shown to produce consistent results in fixed tissue samples decalcified with ethanol, aligning with the sample preparation protocols employed in this study. The NFP staining method was selected for use in the current investigation due to its balance of specificity, clarity, and cost-effectiveness.

Objectives

This study aimed to achieve three objectives. First, it sought to identify the most reliable histological technique for detecting mechanoreceptors in the porcine ACL and to optimize the staining protocol for this model. Second, it aimed to quantify the number of mechanoreceptors present in a healthy porcine ACL. Lastly, it evaluated the reproducibility of the mechanoreceptor counts between two independent examiners.

Chapter 2: Methods

Removal of ligament and Sample Preparation

The ACLs were harvested from the limbs of juvenile farm pigs along with a portion of the tibial and femoral insertions. The anterior distal portion of the ligaments were marked with a suture. The samples were then placed in a cassette and submerged in 10% formalin to fix the tissue. The samples were then sent to the University of New England for cutting and staining. Decalcification was performed using 14% ethylenediaminetetraacetic acid (EDTA) for two weeks, with decalcification confirmation via X-ray. Tissues were embedded in paraffin in a sagittal orientation for sectioning.

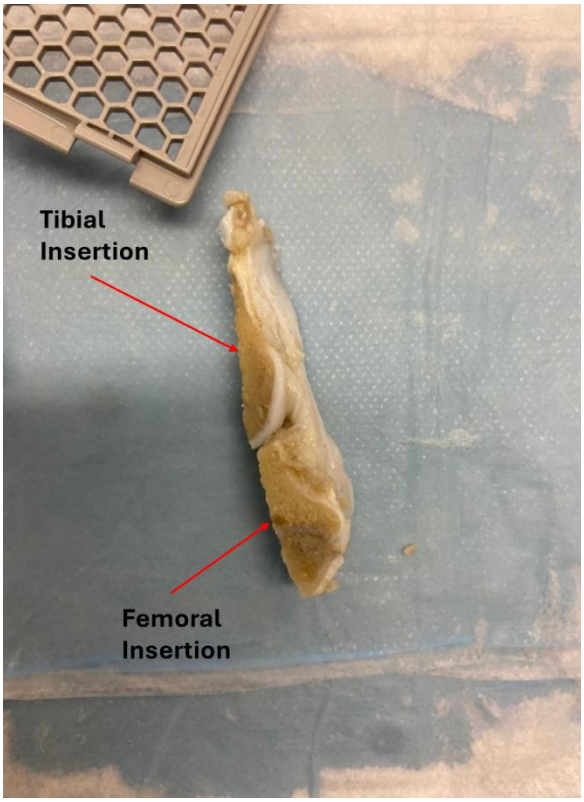

Figure 1: *Porcine ACL samples with portions of the tibial and femoral insertions*

Cutting protocol

The ligament, along with its bony insertions, was sliced in the sagittal plane. Each slice included the entire length and attachment sites of the ligament. 7-micron thick slices were collected at 100-micron intervals across the full span of the ligament insertion and synovium.

This interval was chosen to minimize the risk of overestimating the receptor count, as a smaller gap could result in the same receptor appearing in multiple slices [5].

Neurofilament Protein Staining

The NFP IHC staining technique was optimized by the University of New England (UNE) COBRE Histology and Imaging Core to highlight the mechanoreceptors of the porcine ACL. The optimization was performed using two trial samples. The optimized protocol for the NFP staining was then performed at UNE on one sample as detailed below.

Tissue Preparation and Deparaffinization

Paraffin-embedded porcine ACL sections (7 µm thickness) were deparaffinized by baking at 55°C for 30 minutes, followed by sequential washes in xylene (3 × 3 minutes), 100% ethanol (2 × 1 minute), 95% ethanol (1 × 1 minute), 70% ethanol (30 seconds), and deionized (DI) water until antigen retrieval.

Antigen Retrieval

Heat-induced epitope retrieval (HIER) was performed using citrate buffer (pH 6.0) prepared from a 10X stock solution. Sections were placed in the retrieval solution at room temperature and then incubated in a 55°C water bath overnight (18-20 hours). The following morning, sections were equilibrated to room temperature (RT) for 15-20 minutes and rinsed with DI water (3 × 1 minute).

Peroxidase Blocking

To block endogenous peroxidase activity, sections were incubated in a 3% hydrogen peroxide solution (prepared in methanol) for 10 minutes at RT. After blocking, slides were rinsed with DI water (3 × 1 minute).

Permeabilization and Protein Blocking

Sections were incubated in 0.5% Tween 20 in tris-buffered saline (TBS) for 5 minutes. Excess buffer was removed, and a hydrophobic barrier was drawn around the tissue using a peroxidase-anti-peroxidase (PAP) pen. To reduce nonspecific antibody binding, a 5% normal

donkey serum solution (filtered) in 0.5% TBS-Tween was applied to the sections for 30 minutes at RT.

Primary Antibody Incubation

Neurofilament H (NFH) was detected using a primary antibody (Sigma AB5539) diluted at 1:1500 in blocking solution. The antibody solution (200 µL per slide) was applied, and sections were incubated for 1 hour at RT, protected from light.

Secondary Antibody Incubation

Following primary antibody incubation, slides were washed with 0.5% TBS-Tween (3 × 5 minutes). Donkey anti-chicken IgY HRP-conjugated secondary antibody (Jackson Immunoresearch 703-035-155) was diluted 1:250 in blocking solution and applied for 1 hour at RT, protected from light.

HRP/DAB Substrate Reaction

To visualize antigen-antibody binding, sections were washed in 0.5% TBS-Tween (2 × 5 minutes) followed by a minimum 1-minute incubation in TBS. The 3,3'-diaminobenzidine (DAB) chromogen was prepared by mixing 1 drop of concentrate per 1 mL of buffer. Before chromogen application, slides were washed in DI water for 1 minute. DAB substrate was then applied for 2 minutes, and the reaction was stopped by immersion in DI water. Slides were rinsed in DI water (3 × 1 minute).

Counterstaining

To visualize nuclei, sections were counterstained with Mayer's hematoxylin for 1 minute, followed by sequential washes in DI water (4 × 30 seconds). The nuclei were blued using 0.1% sodium carbonate for 1 minute.

Dehydration and Mounting

Tissue sections were dehydrated through graded ethanol solutions (70% ethanol for 10 seconds, 95% ethanol for 10 seconds, 100% ethanol for 30 seconds × 3), followed by three

washes in xylene (1 minute each). Coverslips were mounted using Cytoseal 60 mounting medium (VWR 48212-154) and allowed to dry before imaging.

Control Staining

To validate the specificity and effectiveness of the staining protocol, control sample staining was conducted using the temporomandibular joint (TMJ) from a rat cranium model. Parasagittal sections, 5 μm in thickness, were prepared and decalcified using a solution of 22% formic acid in 10% sodium citrate. This decalcification protocol was selected to closely mirror the processing conditions used for the porcine ACL samples, ensuring comparable tissue characteristics. The control sections were chosen based on their known abundance of neural structures and stained using the same NFP protocol applied to the porcine ACL tissue. Imaging of the control sample revealed distinct nerve bundles with strong, localized staining. In addition to these large nerve structures, regions with smaller stained fibers were also observed, exhibiting staining characteristics similar to those seen in the porcine ACL sections. This control sample served as a qualitative benchmark for evaluating staining color and intensity.

Histological Imaging and Quantification of Mechanoreceptors

VSI files of 64 slices were obtained using an Olympus VS200 slide scanner. Each entire IHC slice was systematically searched for mechanoreceptors (structures staining positive for NFP antibodies) by two independent reviewers using OlyVIA software (Olympus). A standardized evaluation protocol was followed to ensure consistency in identification and to avoid duplicate counting across slices; detailed criteria and representative examples are provided in Appendix C.

The identification of mechanoreceptors was informed by previously published morphological and dimensional descriptions. Freeman and Wyke's criteria provided initial reference dimensions for common mechanoreceptors: Ruffini endings (approximately 100 × 40 μm), Pacinian corpuscles (approximately 280 × 120 μm), and Golgi tendon organs (approximately 600 × 100 μm) [26]. Additional reference values were drawn from recent literature to supplement this framework. For instance, Wu et al. reported Ruffini endings to be approximately 60 × 25 μm, Pacinian corpuscles around 150 × 40 μm, and Golgi tendon organs

approximately 300 × 70 μm [59]. Sha et al. similarly described Ruffini endings within a range of 50–150 μm and unclassified neural endings ranging from 150–400 μm [35].

These reported size ranges were used as a guide to identify candidate mechanoreceptor structures in the porcine ACL samples, but no attempt was made to classify them into specific mechanoreceptor subtypes. Rather, this literature served to establish reference benchmarks for determining whether a stained structure could be reasonably considered a mechanoreceptor. The goal was solely to quantify the total number of mechanoreceptors observed within the ligament, not to categorize them by type.

Each histological image was initially reviewed at 10× magnification, beginning at the top left corner of the tissue section and moving vertically down each column, proceeding systematically across the entire section. This ensured complete tissue coverage and minimized the likelihood of duplicate identifications. When a structure resembling a mechanoreceptor was identified, a screenshot was taken with the embedded image scale to record its dimensions and facilitate classification verification.

The TMJ control was used throughout the review process to serve as a reference for appropriate staining intensity and coloration. Once a candidate mechanoreceptor exhibited similar staining intensity and hue to the control, its size and morphology were evaluated against the criteria noted above. Additional factors to confirm identification, included:

- Proximity to blood vessels, as mechanoreceptors may be found in association with vasculature but must be distinguished from vascular staining artifacts.
- Tissue location within the section, excluding any structures located within bone, since the focus of this study was on ligament mechanoreceptors.
- Tissue quality, where structures found in poorly preserved or smudged regions were not considered reliable and were excluded from final counts.

All 64 histological sections were reviewed using this standardized and rigorous approach to ensure accurate, reproducible identification of mechanoreceptors within the porcine ACL tissue.

Repeatability Assessment

To assess the repeatability of mechanoreceptor quantification, all the slices of a single porcine ACL were analyzed by two independent examiners. A subset of histological slices (n=23) was designated for training, during which both examiners familiarized themselves with

the identification criteria and methodology. Following this training phase, the remaining slices (n=41) were independently evaluated by each examiner.

The total number of mechanoreceptors identified by each examiner across the slices was recorded, and the percentage of overlap between their counts was used to assess inter-examiner reliability. This comparison was used to quantify the number of mechanoreceptors in the tissue and to evaluate the inter-rater reliability of the identification process.

Chapter 3: Results

The optimized NFP staining protocol successfully labeled mechanoreceptors in the porcine ACL, enabling their visualization and quantification. The final staining protocol is detailed in Appendix 1.

Positive NFP staining indicative of mechanoreceptors was observed in 50 of the 64 slices. The 14 slices that did not have any stained neural structures were concentrated on one end and in the middle of the ligament, between slices 1 and 35. Representative images of the mechanoreceptors are shown in Figure 2 including the first mechanoreceptor identified in slice 5, one from a mid-sagittal slice, and one observed in the final slice. The first four slices did not display any structures with identifiable mechanoreceptor morphology.

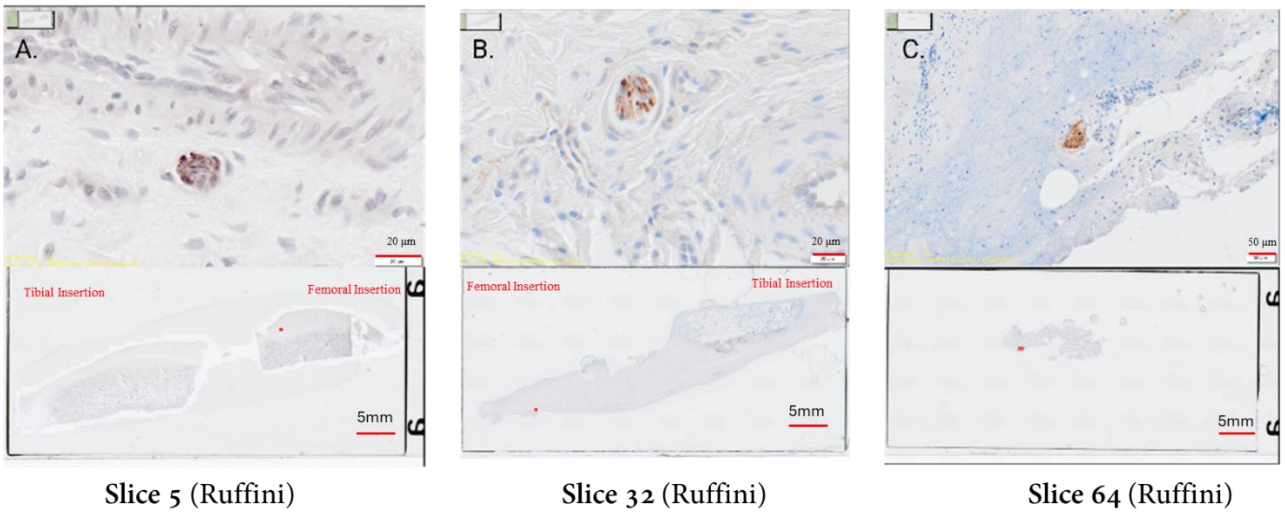

Figure 2: *NFP stained porcine ACL A) First mechanoreceptor identified in slice 5 B) Mechanoreceptor identified in the middle sagittal plane of the ligament, slice 32 C) Mechanoreceptor identified in slice 64*

The first examiner identified a total of 316 mechanoreceptors, while the second examiner identified 539 mechanoreceptors. Despite differences in total count, the distribution patterns across slices showed consistent trends between examiners, as illustrated in Figure 3. The overlap in mechanoreceptor identification between reviewers was calculated at 73.92%, indicating a relatively low level of inter-rater reliability. Specifically, 8 slices exhibited over 95% overlap in identified mechanoreceptors, 11 slices showed over 90% overlap, and 25 slices demonstrated more than 80% overlap. In several slices, particularly in the later part of the series, the second

examiner identified more mechanoreceptors than the first. Across both sets of observations, a consistent trend of increasing mechanoreceptor count was observed along the width of the ligament. The initial 15 slices exhibited low mechanoreceptor counts, with the first examiner identifying between 0 to 4 mechanoreceptors per slice and the second examiner identifying between 0 to 5. Between slices 16 to 39, the first examiner reported between 0 and 9 mechanoreceptors per slice, while the second examiner recorded between 0 and 18. After slice 40, both examiners identified a marked increase in mechanoreceptor counts. In this region, the first examiner noted between 2 and 16 mechanoreceptors per slice, with the highest concentration, 16 mechanoreceptors, observed in slice 46. The second examiner observed between 5 and 31 mechanoreceptors in the same region, with slice 57 showing the maximum of 31 mechanoreceptors.

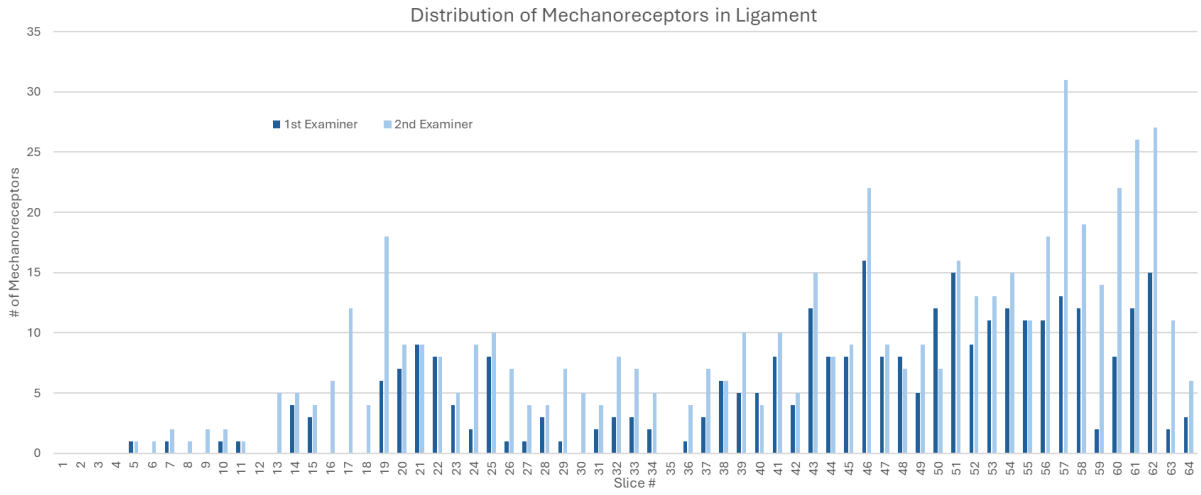

Figure 3: *Distribution of mechanoreceptors per slice along the width of the porcine ligament*

To further analyze spatial distribution, mechanoreceptor localization was evaluated in the context of the insertion-ligament-insertion regions, based on mechanoreceptor identification from the first examiner, as shown in Figure 4. This analysis aimed to examine the distribution of mechanoreceptors across anatomical regions of the ligament. Due to limitations in tissue orientation and sectioning, slices beyond number 47 did not include the complete insertion-ligament-insertion structure and were therefore excluded from this portion of the analysis. In the slices that retained the full anatomical structure, the left insertion region, which is the tibial

attachment site, showed a sparse distribution of mechanoreceptors, with only a few receptors identified. The mid-region of the ligament exhibited a moderate number of mechanoreceptors that were more evenly distributed across the tissue. In contrast, the right insertion site, the femoral attachment site, contained a higher density of mechanoreceptors, particularly clustered near the insertion edge. It is important to note, however, that this mapping represents only 155 mechanoreceptors, less than half of the total 316 mechanoreceptors identified by examiner 1. The remaining 161 mechanoreceptors were concentrated beyond slice 47. As a result, Figure 4 does not fully capture the overall mechanoreceptor distribution within the ligament but rather serves as a representation of the spatial trend across the insertion-ligament-insertion region.

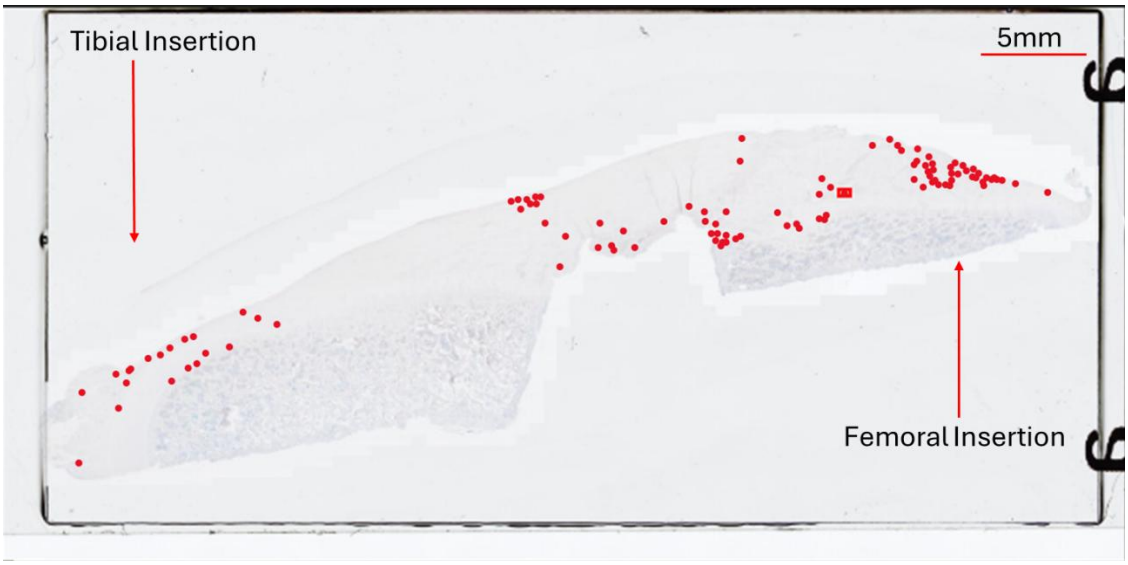

Figure 4: *Spatial distribution of mechanoreceptors mapped across the insertion-ligament-insertion region of the porcine ACL. Red dots represent the locations of mechanoreceptors identified in slices 1–47, overlaid onto the anatomical reference of slice 14 to illustrate overall distribution patterns across the ligament's longitudinal axis*

To complement this analysis, Figure 5 presents the distribution of mechanoreceptors across the insertion-ligament-insertion region in a single representative slice, slice 46. Mechanoreceptors identified by Examiner 1 are marked in red, while those identified by Examiner 2 are shown in blue. This figure highlights both the areas of overlap and differences between examiners, offering insight into inter-examiner variability and emphasizing the potential subjectivity involved in mechanoreceptor identification.

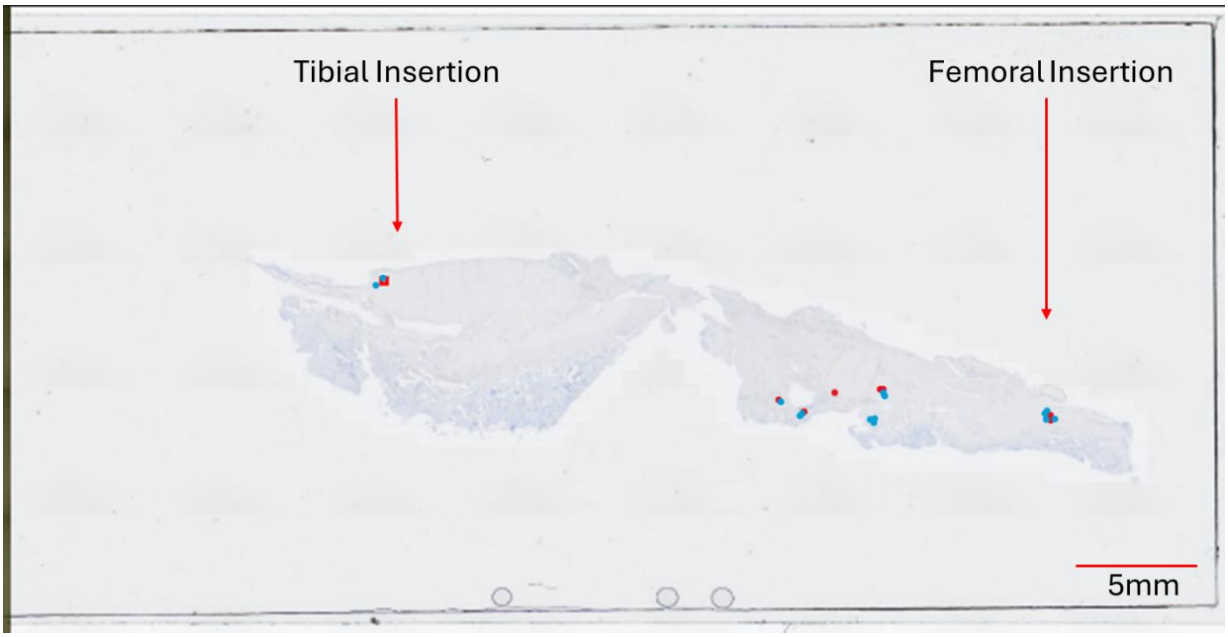

Figure 5: *Distribution of mechanoreceptors across the insertion-ligament-insertion region of slice 46. In red are mechanoreceptors identified by Examiner 1 and in blue are mechanoreceptors identified by Examiner 2*

Chapter 4: Discussion

This analysis revealed the spatial distribution trends across the width of the ligament and over the insertion-ligament-insertion region of each slice and emphasized the critical need to improve the standardization in the criteria used for mechanoreceptor identification.

The distribution of mechanoreceptors across the 64 histological slices of the porcine ACL revealed a non-uniform pattern, characterized by a gradual progression in mechanoreceptor presence across the width of the ligament, from slices 1 to 64. Both examiners observed a consistent trend of increasing mechanoreceptor counts from the early to the later slices, suggesting a spatial pattern in mechanoreceptor localization along the width of the ligament. This trend became most prominent after slice 40, where both examiners noted a marked rise in mechanoreceptor density.

Despite consistency in spatial trends, a notable discrepancy emerged in the absolute number of mechanoreceptors identified by the two examiners. Examiner 2 reported 539 mechanoreceptors, substantially more than the 316 reported by Examiner 1. This difference likely stems from varying interpretations of identification criteria. While both examiners referenced general morphological features and size ranges from the literature, parameters such as staining intensity and color thresholds were not standardized.

Examiner 2 initially aimed to capture all stained regions, without strictly filtering by the aforementioned criteria. After meeting with Examiner 1, they reviewed their selections and discussed each one to come to consensus on what constituted a mechanoreceptor. Examiner 2's counts included faintly stained or ambiguous structures that still fell within a plausible range based on literature descriptions. In contrast, Examiner 1 applied more conservative thresholds, prescreening structures and applying stricter filters when determining mechanoreceptor presence. This variability highlights the interpretive challenges in histological analysis and underscores the need for refined, standardized protocols. Examples of such ambiguous structures accepted by Examiner 2 but excluded by Examiner 1 are shown in Figure 6, highlighting this variability. In panel A, a structure slightly below the accepted size threshold was rejected by Examiner 1 but accepted by Examiner 2 due to its close approximation. In panel B, a faintly stained structure with a single dark region was similarly excluded by Examiner 1 due to insufficient staining intensity but accepted by Examiner 2 in the absence of standardized color and intensity

thresholds within the initial quantification criteria. These examples demonstrate how subtle differences in interpretation can lead to discrepancies in mechanoreceptor quantification.

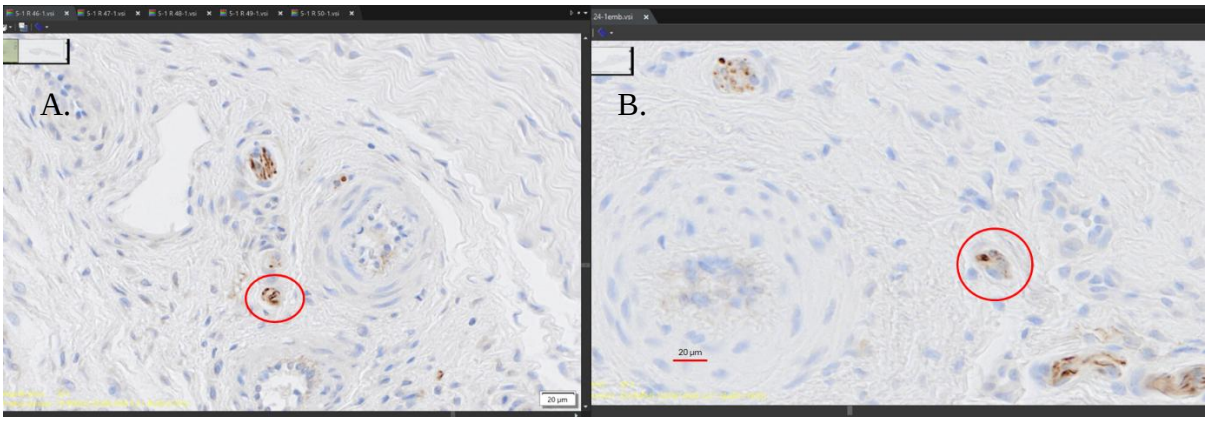

Figure 6: *Example images of ambiguous structures that were accepted as mechanoreceptors by Examiner 2 but rejected by Examiner 1. A. Stained structure (circled in red) in slice 46 measured just under 20 µm and was excluded by Examiner 1 for not meeting the size criterion. Examiner 2 accepted the structure due to its close proximity to the lower size threshold. B. Stained structure (circled in red) in slice 24 displayed overall light staining with only a single dark focal point, leading to its rejection by Examiner 1. Examiner 2 accepted the structure due to the absence of standardized color and intensity threshold.*

To investigate the modest initial overlap of 73.9%, Examiner 1 re-evaluated slices where they had initially identified few or no mechanoreceptors. After reviewing Examiner 2's selections, Examiner 1 recounted mechanoreceptors per slice, resulting in a new total of 429 and increasing inter-examiner overlap to 88.6%, as shown in Figure 7. This improvement suggests that standardized, stringent criteria could significantly improve consistency between observers. Additional evaluations based on the new criteria will be performed on an additional set of porcine ACLs.

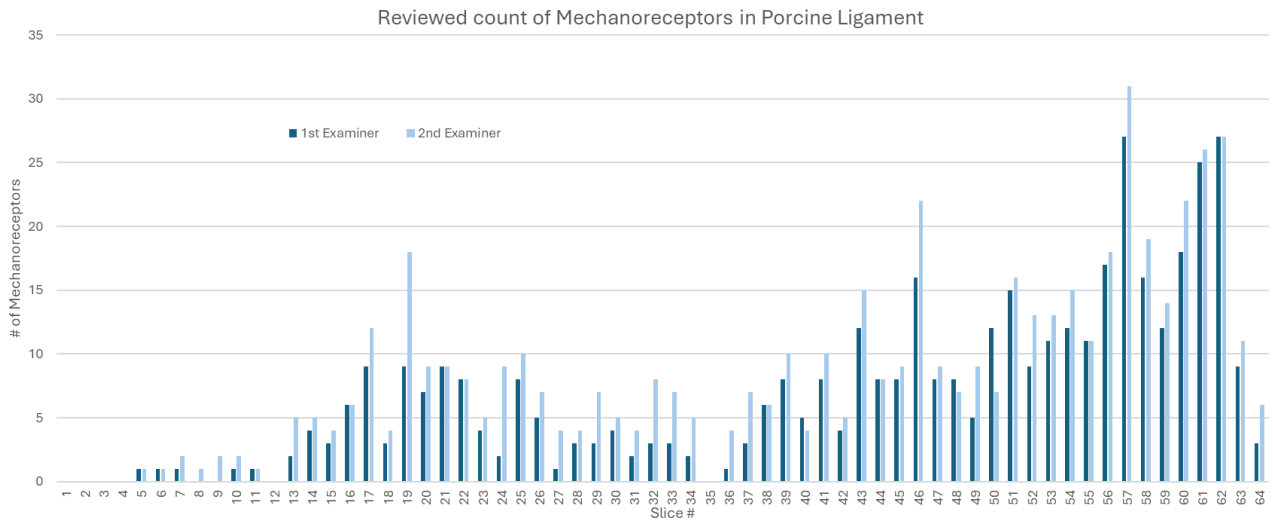

Figure 7: *Re-evaluated mechanoreceptor counts across ligament slices by Examiner 1. Following re-examination, counts were adjusted to reflect improved alignment and highlight inter-examiner consistency across the ligament's length*

Detection variability may also arise from the lack of standardized definitions in the literature regarding what precisely constitutes a mechanoreceptor. Primary studies often differ in their descriptions of mechanoreceptor morphology, and many do not clearly report key methodological details such as tissue orientation, sectioning angle, and slice intervals [26, 35]. In some cases, these factors are not mentioned at all, which adds ambiguity to structural interpretation [26]. As mechanoreceptor appearance can vary significantly depending on these parameters, this inconsistency likely contributed to the initial discrepancy in counts. Nonetheless, both datasets in this study demonstrated consistent spatial distribution, supporting the reliability of the observed pattern of greater mechanoreceptor distribution in the mid-to-end regions of the ligament.

To improve reliability in future studies, it is critical to establish rigorous, objective identification protocols. These improvements would include developing precise morphological definitions, apply consistent size constraints, and establishing quantitative staining intensity thresholds, potentially supported by a reference dataset with confirmed mechanoreceptor examples. In addition to established criteria such as proximity to vasculature, anatomical location within the tissue, and overall section quality, it is critical to assess whether mechanoreceptor-like structures appearing in the same spatial coordinates across serial sections represent a single

sagittally sectioned nerve fiber. Properly accounting for this ensures accurate mechanoreceptor quantification.

Compared to existing literature, the total number of mechanoreceptors identified in this study is substantially higher. Banios et al. reported a median of 18 mechanoreceptors per ACL remnant in 29 human samples [14], Sha et al. found 106 mechanoreceptors across 60 human tibial ACL remnants [35], and Gao et al. identified 318 mechanoreceptors in 40 human ACL remnants [60]. While these assessments did not include the entire ligament, these relatively low counts may reflect challenges specific to human tissue, such as degradation in torn remnants and/or limitations in staining quality. Additionally, if the mechanoreceptors quantified in these studies were counted over only a small portion of the original ligament, the total number of mechanoreceptors in a healthy, intact human ACL may not differ substantially from the counts observed in this study in healthy porcine ACLs. Furthermore, this study analyzed intact porcine ACLs, allowing for more comprehensive sectioning and staining.

Comparisons to other animal models further highlight the differences in mechanoreceptor counts. In a rat model, a median of 17 mechanoreceptors per healthy ACL was reported [61], while in a sheep model, a median of 27 mechanoreceptors per healthy ACL was identified [62]. Although the mechanoreceptor counts found in the porcine model are substantially higher than those observed in the rat and sheep models, the anatomical and biomechanical similarities between porcine and human ACLs suggest that porcine ligament mechanoreceptor counts may provide a closer approximation to the true mechanoreceptor density in healthy human tissue.

Therefore, although the repeatability of our mechanoreceptor counts remains limited by identification criteria, the higher counts reported here may serve as a more accurate benchmark for healthy ligament innervation. Our findings underscore the potential underestimation of mechanoreceptor presence in injured or remnant human tissues, which are often used as the basis for prior quantification efforts.

Understanding mechanoreceptor distribution across the insertion-ligament-insertion regions provides critical insight into the neurosensory function of the ACL. Localizing mechanoreceptors within this anatomical context is essential for identifying areas of neural innervation, which has implications for understanding native ligament function, the impact of injury, and the potential for reinnervation following reconstruction. In particular, characterizing

regions with the highest mechanoreceptor density can help determine whether innervation patterns in healing or reconstructed ACLs recapitulate those of the native ligament.

In this study, spatial localization across the insertion-ligament-insertion area was based solely on Examiner 1's initial findings due to time constraints and was limited to slices 1-47 which retained the full insertion-ligament-insertion structure. Beyond slice 47, the insertion-ligament-insertion structure was no longer preserved, precluding accurate mapping of mechanoreceptor locations in these later slices. Notably, this section, slices 48 to 64, of the ligament contained a higher number of mechanoreceptors overall. As such, only 155 mechanoreceptors were mapped in Figure 4, while the remaining 161 mechanoreceptors identified by Examiner 1 were excluded from the spatial analysis. This is a key limitation, as the incomplete dataset likely underrepresents areas of highest mechanoreceptor density and hinders the ability to fully characterize their anatomical distribution.

Nonetheless, the available data revealed meaningful trends. As seen in figure 4, the tibial attachment site exhibited a lower concentration of mechanoreceptors compared to the femoral end, potentially indicating reduced neural innervation at this site. In contrast, the central region of the ligament, in figure 4, showed a moderate and evenly spaced distribution of mechanoreceptors, suggesting active proprioceptive signaling along the ligament body during joint movement. The femoral attachment site demonstrated the highest mechanoreceptor density, in figure 4, with receptors densely clustered near the insertion edge, implying rich innervation that may be functionally significant. These findings are consistent with previous studies reporting higher mechanoreceptor density at ligament attachment sites in both human and animal models [14, 61-64], supporting the hypothesis that these regions are critical for proprioception. However, prior studies did not note any distinct distribution differences between the attachment sites [63, 64]. This could either reflect incomplete data reporting or represent a potential trend worth further investigation. Notably, 43% of ACL tears occur at the femoral insertion site [65]; given the greater mechanoreceptor density observed at this location in the current study, such injuries may result in a disproportionately large loss of neural elements. Similarly, 52% of ACL tears occur in the midsubstance of the ligament [65], where a moderate concentration of mechanoreceptors was observed in this study. Damage in these regions would likely impair proprioceptive signaling, further emphasizing the clinical importance of understanding regional

mechanoreceptor distribution. These observations highlight the potential impact of injury location on neurosensory function and the importance of targeted rehabilitation strategies.

To improve spatial accuracy in future studies, it is essential to map each histological slice to a sagittal reference image of the full insertion-ligament-insertion structure. Doing so would ensure that the precise anatomical location of each slice is documented, thereby enabling more accurate localization of mechanoreceptors along the ligament and allowing for a comprehensive analysis of distribution trends across the entire ligament.

Although the mapped dataset does not fully represent the entire ligament, it offers valuable insight into mechanoreceptor localization patterns. The observed clustering at both ends of the ligament, along with moderate presence in the central region, supports the hypothesis that mechanoreceptors are strategically distributed to facilitate proprioceptive feedback across the ACL. These findings carry important implications for surgical reconstruction and rehabilitation, as preserving or replicating this spatial distribution may be key to restoring neurosensory function.

Several limitations were encountered during the execution of this study. One of the primary challenges was the need for multiple iterations to optimize the staining protocols for the porcine ACL samples. We are confident that the final NFP protocol will be valuable for future studies. Another limitation was the small sample size, as time constraints allowed for the evaluation of only one ligament. While the NFP successfully labeled mechanoreceptors, artifact staining of vasculature was observed in some sections, as shown in Figure 8. These artifacts appeared as darkly stained structures but did not meet Freeman and Wyke's classification criteria [26] for mechanoreceptors, allowing for their exclusion from the final analysis. This artifact staining may have resulted from the close anatomical relationship between nerves and blood vessels, where endothelial cells may have inadvertently absorbed the stain. Additionally, as the slices progressed through the ligament, image and tissue quality deteriorated due to a reduction in viable ligamentous material available for histological analysis, which may have further limited mechanoreceptor identification in certain regions. Lastly, only a single staining technique was used in this study. The addition of a complementary method, such as S-100, could enhance mechanoreceptor visualization and help validate the specificity of staining, thereby minimizing potential misidentification.

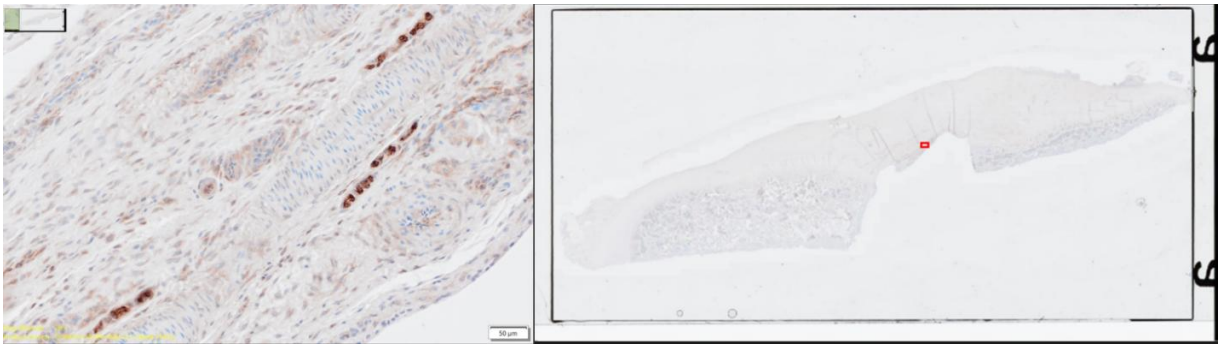

Figure 8: *NFP Stained artifacts resembling vascular structures observed in porcine ligament tissue sections, slice 18*

Despite these limitations, this study successfully established a robust mechanoreceptor staining and identification protocol that can be utilized in future investigations. To further enhance the accuracy of mechanoreceptor identification, co-labeling with S-100 could be optimized to complement NFP staining. In our hands, staining with S-100 alone was less specific than NFP. However, the combination has been used successfully [19, 30, 31]. Refining the S-100 staining method may increase the likelihood of correctly identifying mechanoreceptors by providing additional morphological confirmation. Efforts to optimize this co-labeling approach are ongoing, as illustrated in Figure 9, which presents preliminary fluorescent immunohistochemistry results showing NFP-S-100 co-labeled mechanoreceptors in the porcine ACL.

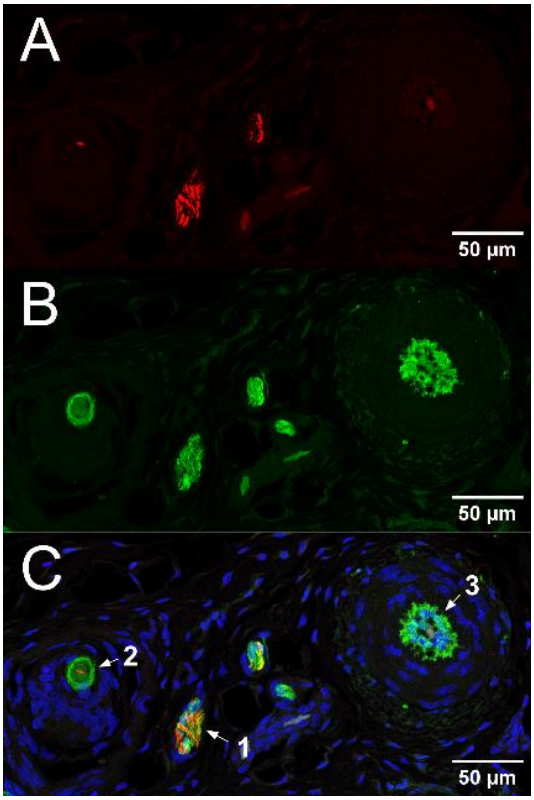

Figure 9: *Example of fluorescent co-labeled NFP and S-100 IHC highlighting mechanoreceptors of the porcine ACL (200X). A) red NFP positive structures. B) green S100 positive structures. C) Overlay of NFP-red, S-100-green, and DAPI(4',6-diamidino-2-phenylindole)-blue, highlighting mechanoreceptor structures co-labeled with NFP and S-100. Objects 1 and 2 are mechanoreceptors and Object 3 is a vessel, which is also stained with S-100.*

Moving forward, the next steps involve assessing five porcine ACLs to evaluate inter-examiner reliability across a larger sample size using the co-labeling of S-100 with NFP and using refined identification criteria. Additionally, efforts will be directed toward developing a protocol to assess mechanoreceptor function following BEAR and ACL reconstruction using an impact loading system designed to trigger the hamstring-ACL reflex arc [66]. This protocol was inspired by Freimert et al., who conducted a similar study of the normal ACL in humans under general anesthesia [66]. Currently, our method involves a weight-and-pulley system, where one end of the system is attached to the ACL, while the other end holds a suspended weight that is dropped from a predetermined height to induce mechanoreceptor activation. The latency of the ACL-hamstring reflex arc will be measured to determine the differences in mechanoreceptor function between healthy ACLs, reconstructed ACLs, and BEAR ACLs in a pre-clinical model. A diagram of this loading system is provided in Appendix 2.

Conclusion

Given the high prevalence of ACL injuries, it is essential to understand the consequences of ligament disruption on neuromuscular function and proprioception. This study provides foundational anatomical and methodological insights into the total count and spatial distribution of mechanoreceptors in a healthy, native porcine ACL, mapped both along the insertion-ligament-insertion axis and across the ligament's width. While further refinement is needed to improve the reliability of mechanoreceptor quantification, the findings offer a baseline for future comparisons with ACL grafts and BEAR-repaired tissues. Understanding whether mechanoreceptor density and organization are restored following surgical intervention is critical for evaluating the ability of grafts to reestablish sensory function and overall ligament integrity. This work also presents an optimized staining approach for mechanoreceptor detection and contributes valuable data to the field of ligament neurobiology.

References

[1] C. B. Frank, "Ligament structure, physiology and function," (in eng), *J Musculoskelet Neuronal Interact*, vol. 4, no. 2, pp. 199-201, Jun 2004.

[2] IQWiG, *In brief: What are ligaments?* NCBI Bookshelf: Institute for Quality and Efficiency in Health Care (IQWiG), Cologne, Germany, 2019.

[3] E. Hagert, M. Garcia-Elias, S. Forsgren, and B.-O. Ljung, "Immunohistochemical Analysis of Wrist Ligament Innervation in Relation to Their Structural Composition," *The Journal of Hand Surgery*, vol. 32, no. 1, pp. 30-36, 2007/01/01/ 2007, doi: https://doi.org/10.1016/j.jhsa.2006.10.005.

[4] D. Adriansyah, A. Santoso, T. S. Sibarani, and N. A. Setyawan, "Mechanoreceptor analysis on femoral and tibial site remnant of anterior cruciate ligament injury using immunohistochemistry," *Ann Med Surg (Lond)*, vol. 78, p. 103849, Jun 2022, doi: 10.1016/j.amsu.2022.103849.

[5] S. W. Young, R. D. Valladares, F. Loi, and J. L. Dragoo, "Mechanoreceptor Reinnervation of Autografts Versus Allografts After Anterior Cruciate Ligament Reconstruction," *Orthop J Sports Med*, vol. 4, no. 10, p. 2325967116668782, Oct 2016, doi: 10.1177/2325967116668782.

[6] H. Fujie, "Mechanical Properties and Biomechanical Function of the ACL," in *ACL Injury and Its Treatment*, M. Ochi, K. Shino, K. Yasuda, and M. Kurosaka Eds. Tokyo: Springer Japan, 2016, pp. 69-77.

[7] M. R. Krogsgaard, T. Fischer-Rasmussen, and P. Dyhre-Poulsen, "Absence of sensory function in the reconstructed anterior cruciate ligament," (in eng), *J Electromyogr Kinesiol*, vol. 21, no. 1, pp. 82-6, Feb 2011, doi: 10.1016/j.jelekin.2010.09.012.

[8] Stanford, "Knee Ligament Injury: Causes." [Online]. Available: https://stanfordhealthcare.org/medical-conditions/bones-joints-and-muscles/knee-ligament-injury/causes.html

[9] MayoClinic, "ACL Injury - Symptoms and Causes." [Online]. Available: https://www.mayoclinic.org/diseases-conditions/acl-injury/symptoms-causes/syc-20350738

[10] T. N. Vitharana, E. King, and K. Moran, "Sensorimotor Dysfunction Following Anterior Cruciate Ligament Reconstruction- an Afferent Perspective: A Scoping Review," *Int J Sports Phys Ther*, vol. 19, no. 1, pp. 1410-1437, 2024, doi: 10.26603/001c.90862.

[11] G. N. Williams, P. J. Barrance, L. Snyder-Mackler, and T. S. Buchanan, "Altered quadriceps control in people with anterior cruciate ligament deficiency," *Med Sci Sports Exerc*, vol. 36, no. 7, pp. 1089-97, Jul 2004, doi: 10.1249/01.mss.0000131959.20666.11.

[12] P. Dougherty, "Somatosensory Systems," *Neuroscience Online*: University Texas Health, Department of Neurobiology and Anatomy, 2020. [Online]. Available: https://nba.uth.tmc.edu/neuroscience/m/s2/chapter02.html

[13] P. Jooya and F. Delavari, "The Proprioceptive System," in *Biophysics and Neurophysiology of the Sixth Sense*, N. Rezaei and A. Saghazadeh Eds. Cham: Springer International Publishing, 2019, pp. 85-98.

[14] K. Banios, V. Raoulis, A. Fyllos, D. Chytas, V. Mitrousias, and A. Zibis, "Anterior and Posterior Cruciate Ligaments Mechanoreceptors: A Review of Basic Science," (in eng), *Diagnostics (Basel)*, vol. 12, no. 2, Jan 27 2022, doi: 10.3390/diagnostics12020331.

[15] F. Iheanacho and A. R. Vellipuram, "Physiology, Mechanoreceptors." [Online]. Available: https://www.ncbi.nlm.nih.gov/books/NBK541068/

[16] L. Thau, V. Reddy, and P. Singh, "Anatomy, Central Nervous System." [Online]. Available: https://www.ncbi.nlm.nih.gov/books/NBK542179/

[17] R. A. Schultz, D. C. Miller, C. S. Kerr, and L. Micheli, "Mechanoreceptors in human cruciate ligaments. A histological study," (in eng), *J Bone Joint Surg Am*, vol. 66, no. 7, pp. 1072-6, Sep 1984.

[18] M. L. Zimny and C. S. Wink, "Neuroreceptors in the tissues of the knee joint," (in eng), *J Electromyogr Kinesiol*, vol. 1, no. 3, pp. 148-57, Sep 1991, doi: 10.1016/1050-6411(91)90031-y.

[19] Y. H. Han, B. Li, and Y. Wen, "Distribution, quantity and gene expression of mechanoreceptors in ligaments and tendons of knee joint in rabbits," (in eng), *J Mol Histol*, vol. 51, no. 3, pp. 233-240, Jun 2020, doi: 10.1007/s10735-020-09875-8.

[20] J. Nyland, C. Gamble, T. Franklin, and D. N. M. Caborn, "Permanent knee sensorimotor system changes following ACL injury and surgery," (in eng), *Knee Surg Sports*

Traumatol Arthrosc, vol. 25, no. 5, pp. 1461-1474, May 2017, doi: 10.1007/s00167-017-4432-y.

[21] E. Tsuda, Y. Okamura, H. Otsuka, T. Komatsu, and S. Tokuya, "Direct evidence of the anterior cruciate ligament-hamstring reflex arc in humans," *Am J Sports Med*, vol. 29, no. 1, pp. 83-7, Jan-Feb 2001, doi: 10.1177/03635465010290011801.

[22] D. G. Stuart, G. E. Goslow, C. G. Mosher, and R. M. Reinking, "Stretch responsiveness of Golgi tendon organs," (in eng), *Exp Brain Res*, vol. 10, no. 5, pp. 463-76, Jun 25 1970, doi: 10.1007/bf00234263.

[23] J. Houk and W. Simon, "Responses of Golgi tendon organs to forces applied to muscle tendon," (in eng), *J Neurophysiol*, vol. 30, no. 6, pp. 1466-81, Nov 1967, doi: 10.1152/jn.1967.30.6.1466.

[24] R. M. Biedert and E. B. Zwick, "Ligament-muscle reflex arc after anterior cruciate ligament reconstruction: electromyographic evaluation," *Arch Orthop Trauma Surg*, vol. 118, no. 1-2, pp. 81-4, 1998, doi: 10.1007/s004020050317.

[25] D. Deflorio, M. Di Luca, and A. M. Wing, "Skin and Mechanoreceptor Contribution to Tactile Input for Perception: A Review of Simulation Models," (in eng), *Front Hum Neurosci*, vol. 16, p. 862344, 2022, doi: 10.3389/fnhum.2022.862344.

[26] M. A. Freeman and B. Wyke, "The innervation of the knee joint. An anatomical and histological study in the cat," (in eng), *J Anat*, vol. 101, no. Pt 3, pp. 505-32, Jun 1967.

[27] C. Germann, R. Sutter, and D. Nanz, "Novel observations of Pacinian corpuscle distribution in the hands and feet based on high-resolution 7-T MRI in healthy volunteers," (in eng), *Skeletal Radiol*, vol. 50, no. 6, pp. 1249-1255, Jun 2021, doi: 10.1007/s00256-020-03667-7.

[28] T. HOGERVORST and R. A. BRAND, "Current Concepts Review - Mechanoreceptors in Joint Function*," *JBJS*, vol. 80, no. 9, pp. 1365-1378, 1998. [Online]. Available: https://journals.lww.com/jbjsjournal/fulltext/1998/09000/current_concepts_review___mechanoreceptors_in.18.aspx.

[29] B. Li, Y. T. Wang, L. H. Bai, and Y. Wen, "Changes of mechanoreceptors in different-state remnants of ruptured anterior cruciate ligament," (in eng), *Int Orthop*, vol. 42, no. 11, pp. 2613-2618, Nov 2018, doi: 10.1007/s00264-018-3933-8.

[30] H. Çabuk, F. Kuşku Çabuk, and K. Turan, "The time from injury to surgery is an important factor affecting the mechanoreceptors at stump of torn anterior cruciate ligament," *Archives of Orthopaedic and Trauma Surgery*, vol. 142, no. 11, pp. 3389-3393, 2022/11/01 2022, doi: 10.1007/s00402-021-04310-3.

[31] M. S. Dhillon, K. Bali, and R. K. Vasistha, "Immunohistological evaluation of proprioceptive potential of the residual stump of injured anterior cruciate ligaments (ACL)," (in eng), *Int Orthop*, vol. 34, no. 5, pp. 737-41, Jun 2010, doi: 10.1007/s00264-009-0948-1.

[32] M. Goertzen, J. Gruber, A. Dellmann, H. Clahsen, and K. P. Schulitz, "Neurohistological findings after experimental anterior cruciate ligament allograft transplantation," *Archives of Orthopaedic and Trauma Surgery*, vol. 111, no. 2, pp. 126-129, 1992/02/01 1992, doi: 10.1007/BF00443480.

[33] B. I. Lee *et al.*, "Immunohistochemical study of mechanoreceptors in the tibial remnant of the ruptured anterior cruciate ligament in human knees," *Knee Surgery, Sports Traumatology, Arthroscopy*, vol. 17, no. 9, pp. 1095-1101, 2009/09/01 2009, doi: 10.1007/s00167-009-0831-z.

[34] A. D. Georgoulis *et al.*, "The presence of proprioceptive mechanoreceptors in the remnants of the ruptured ACL as a possible source of re-innervation of the ACL autograft," (in eng), *Knee Surg Sports Traumatol Arthrosc*, vol. 9, no. 6, pp. 364-8, Nov 2001, doi: 10.1007/s001670100240.

[35] L. Sha, G. Xie, S. Zhao, and J. Zhao, "A morphologic and quantitative comparison of mechanoreceptors in the tibial remnants of the ruptured human anterior cruciate ligament," (in eng), *Medicine (Baltimore)*, vol. 96, no. 5, p. e6081, Feb 2017, doi: 10.1097/md.0000000000006081.

[36] N. Adachi, M. Ochi, Y. Uchio, J. Iwasa, K. Ryoke, and M. Kuriwaka, "Mechanoreceptors in the anterior cruciate ligament contribute to the joint position sense," (in eng), *Acta Orthop Scand*, vol. 73, no. 3, pp. 330-4, Jun 2002, doi: 10.1080/00016470232015356.

[37] C. Hulet *et al.*, "The use of allograft tendons in primary ACL reconstruction," *Knee Surgery, Sports Traumatology, Arthroscopy*, vol. 27, no. 6, pp. 1754-1770, 2019/06/01 2019, doi: 10.1007/s00167-019-05440-3.

[38] Y. Wada, T. Takahashi, Y. Michinaka, Y. Morisawa, and H. Yamamoto, "Mechanoreceptors of patellar tendon used for ACL reconstruction. Rabbit experiments," (in eng), *Acta Orthop Scand,* vol. 68, no. 6, pp. 559-62, Dec 1997, doi: 10.3109/17453679708999026.

[39] S. H. Kim, C. H. Chun, K. C. Chun, H. J. Jo, and K. M. Kim, "Histological assessment of mechanoreceptors in Achilles allografts after anterior cruciate ligament reconstruction," (in eng), *Am J Sports Med,* vol. 40, no. 9, pp. 2061-5, Sep 2012, doi: 10.1177/0363546512453303.

[40] M. M. Murray *et al.*, "Bridge-Enhanced Anterior Cruciate Ligament Repair: Two-Year Results of a First-in-Human Study," *Orthopaedic Journal of Sports Medicine,* vol. 7, no. 3, p. 2325967118824356, 2019, doi: 10.1177/2325967118824356.

[41] K. Bali, M. S. Dhillon, R. K. Vasistha, N. Kakkar, R. Chana, and S. Prabhakar, "Efficacy of immunohistological methods in detecting functionally viable mechanoreceptors in the remnant stumps of injured anterior cruciate ligaments and its clinical importance," (in eng), *Knee Surg Sports Traumatol Arthrosc,* vol. 20, no. 1, pp. 75-80, Jan 2012, doi: 10.1007/s00167-011-1526-9.

[42] A. L. Bascunan, A. Biedrzycki, S. A. Banks, D. D. Lewis, and S. E. Kim, "Large Animal Models for Anterior Cruciate Ligament Research," *Front Vet Sci,* vol. 6, p. 292, 2019, doi: 10.3389/fvets.2019.00292.

[43] Q. Shi, H. Wang, K. He, M. Tao, and C.-K. Cheng, "Comparison of the morphology of the anterior cruciate ligament and related bony structures between pigs and humans," (in English), *Frontiers in Veterinary Science,* Original Research vol. Volume 9 - 2022, 2022-November-18 2022, doi: 10.3389/fvets.2022.1045785.

[44] J. M. O'Donnell, B. M. Devitt, and M. Arora, "The role of the ligamentum teres in the adult hip: redundant or relevant? A review," *J Hip Preserv Surg,* vol. 5, no. 1, pp. 15-22, Jan 2018, doi: 10.1093/jhps/hnx046.

[45] D. Rebmann, H. O. Mayr, H. Schmal, S. Hernandez Latorre, and A. Bernstein, "Immunohistochemical analysis of sensory corpuscles in human transplants of the anterior cruciate ligament," *J Orthop Surg Res,* vol. 15, no. 1, p. 270, Jul 17 2020, doi: 10.1186/s13018-020-01785-5.

[46] J. R. Gosney, "2 - Identification, morphology and secretory products of the pulmonary endocrine system," in *Pulmonary Endocrine Pathology*, J. R. Gosney Ed.: Butterworth-Heinemann, 1992, pp. 6-24.

[47] K. C. Chun, S. H. Lee, J. W. Kim, E. J. Jin, K. M. Kim, and C. H. Chun, "Immunohistochemical and immunocytochemical study of mechanoreceptors in anterior cruciate ligament reconstruction with the remnant-preserving technique using Achilles tendon allografts," *J Orthop Surg Res*, vol. 12, no. 1, p. 93, Jun 14 2017, doi: 10.1186/s13018-017-0593-0.

[48] J. Chen and S. Chen, "Relationship Between Mechanoreceptors in the Posterior Cruciate Ligament and Patient Age or Osteoarthritis Severity," *Orthopaedic Journal of Sports Medicine*, vol. 11, no. 6, p. 23259671231168894, 2023, doi: 10.1177/23259671231168894.

[49] M. Nayak, H. L. Nag, S. Gaba, T. C. Nag, and S. Sharma, "Quantitative correlation of mechanoreceptors in tibial remnant of ruptured human anterior cruciate ligament with duration of injury and its significance: an immunohistochemistry-based observational study," *J Orthop Traumatol*, vol. 19, no. 1, p. 5, Jul 18 2018, doi: 10.1186/s10195-018-0498-7.

[50] R. Krauspe, F. Schmitz, G. Zoller, and D. Drenckhahn, "Distribution of neurofilament-positive nerve fibres and sensory endings in the human anterior cruciate ligament," *Arch Orthop Trauma Surg*, vol. 114, no. 4, pp. 194-8, 1995, doi: 10.1007/BF00444261.

[51] B. Fromm, B. Schafer, D. Parsch, and W. Kummer, "Reconstruction of the anterior cruciate ligament with a cyropreserved ACL allograft. A microangiographic and immunohistochemical study in rabbits," *Int Orthop*, vol. 20, no. 6, pp. 378-82, 1996, doi: 10.1007/s002640050102.

[52] M. D. McGavin, "Factors affecting visibility of a target tissue in histologic sections," *Vet Pathol*, vol. 51, no. 1, pp. 9-27, Jan 2014, doi: 10.1177/0300985813506916.

[53] L. K. Campbell, J. R. Thomas, L. W. Lamps, B. R. Smoller, and A. L. Folpe, "Protein Gene Product 9.5 (PGP 9.5) Is Not a Specific Marker of Neural and Nerve Sheath Tumors: An Immunohistochemical Study of 95 Mesenchymal Neoplasms," *Modern Pathology*, vol. 16, no. 10, pp. 963-969, 2003/10/01 2003, doi: 10.1097/01.MP.0000087088.88280.B0.

[54] A. B. Kanik, M. Yaar, and J. Bhawan, "p75 nerve growth factor receptor staining helps identify desmoplastic and neurotropic melanoma," *J Cutan Pathol,* vol. 23, no. 3, pp. 205-10, Jun 1996, doi: 10.1111/j.1600-0560.1996.tb01468.x.

[55] A. Franchi, G. Zaccherotti, and P. Aglietti, "Neural system of the human posterior cruciate ligament in osteoarthritis," *J Arthroplasty,* vol. 10, no. 5, pp. 679-82, Oct 1995, doi: 10.1016/s0883-5403(05)80215-3.

[56] M. J. Schutte, E. J. Dabezies, M. L. Zimny, and L. T. Happel, "Neural anatomy of the human anterior cruciate ligament," *J Bone Joint Surg Am,* vol. 69, no. 2, pp. 243-7, Feb 1987. [Online]. Available: https://www.ncbi.nlm.nih.gov/pubmed/3805085.

[57] J. W. Witherspoon, I. V. Smirnova, and T. E. McIff, "Improved gold chloride staining method for anatomical analysis of sensory nerve endings in the shoulder capsule and labrum as examples of loose and dense fibrous tissues," (in eng), *Biotech Histochem,* vol. 89, no. 5, pp. 355-70, Jul 2014, doi: 10.3109/10520295.2013.872297.

[58] P. G. Katonis, A. P. Assimakopoulos, M. V. Agapitos, and E. I. Exarchou, "Mechanoreceptors in the posterior cruciate ligament. Histologic study on cadaver knees," *Acta Orthop Scand,* vol. 62, no. 3, pp. 276-8, Jun 1991, doi: 10.3109/17453679108993609.

[59] X. Wu, W. Song, C. Zheng, S. Zhou, and S. Bai, "Morphological study of mechanoreceptors in collateral ligaments of the ankle joint," *J Orthop Surg Res,* vol. 10, p. 92, Jun 12 2015, doi: 10.1186/s13018-015-0215-7.

[60] F. Gao *et al.*, "A Morphologic and Quantitative Study of Mechanoreceptors in the Remnant Stump of the Human Anterior Cruciate Ligament," *Arthroscopy,* vol. 32, no. 2, pp. 273-80, Feb 2016, doi: 10.1016/j.arthro.2015.07.010.

[61] N. Kanemura *et al.*, "Changes of Mechanoreceptor in Anterior Cruciate Ligament with Hindlimb Suspension Rats," *Journal of Physical Therapy Science,* vol. 14, pp. 27-32, 2002.

[62] J. Raunest, M. Sager, and E. Burgener, "Proprioception of the cruciate ligaments: receptor mapping in an animal model," *Arch Orthop Trauma Surg,* vol. 118, no. 3, pp. 159-63, 1998, doi: 10.1007/s004020050338.

[63] H. Çabuk and F. Kuşku Çabuk, "Mechanoreceptors of the ligaments and tendons around the knee," *Clinical Anatomy*, vol. 29, no. 6, pp. 789-795, 2016, doi: https://doi.org/10.1002/ca.22743.

[64] E. Kholinne *et al.*, "Mechanoreceptors distribution in the human medial collateral ligament of the elbow," *Orthop Traumatol Surg Res*, vol. 104, no. 2, pp. 251-255, Apr 2018, doi: 10.1016/j.otsr.2018.01.005.

[65] J. P. van der List, D. N. Mintz, and G. S. DiFelice, "The Location of Anterior Cruciate Ligament Tears: A Prevalence Study Using Magnetic Resonance Imaging," *Orthop J Sports Med*, vol. 5, no. 6, p. 2325967117709966, Jun 2017, doi: 10.1177/2325967117709966.

[66] B. Friemert, M. Faist, C. Spengler, H. Gerngross, L. Claes, and M. Melnyk, "Intraoperative direct mechanical stimulation of the anterior cruciate ligament elicits short- and medium-latency hamstring reflexes," *J Neurophysiol*, vol. 94, no. 6, pp. 3996-4001, Dec 2005, doi: 10.1152/jn.00410.2005.

[67] R. Cobo *et al.*, "Verification and characterisation of human digital Ruffini's sensory corpuscles," *J Anat*, vol. 238, no. 1, pp. 13-19, Jan 2021, doi: 10.1111/joa.13301.

[68] B. Li, X. D. Luo, and Y. Wen, "Changes in mechanoreceptors in rabbits' anterior cruciate ligaments with age," *J Mol Histol*, vol. 50, no. 3, pp. 229-237, Jun 2019, doi: 10.1007/s10735-019-09820-4.

[69] Z. Halata, "The ultrastructure of the sensory nerve endings in the articular capsule of the knee joint of the domestic cat (Ruffini corpuscles and Pacinian corpuscles)," *J Anat*, vol. 124, no. Pt 3, pp. 717-29, Dec 1977. [Online]. Available: https://www.ncbi.nlm.nih.gov/pubmed/604339.

Appendix A

University of New England NFP Staining Protocol

IHC – Chromogenic (HRP) Detection

Neurofilament H on porcine ACL/bone 7 microns (EDTA decalcified)

Materials and Reagents

- 0.5% Tween 20 in 1X TBS
- 1X tris buffered saline (TBS) pH 7.4, from 10X stock (Corning 46-012-CM)
- Tween 20 (Sigma P9416)
- 3% hydrogen peroxide in methanol
- 30% Hydrogen Peroxide (Sigma-Aldrich 216763-500ML) o Methanol (Sigma 34860-2L-R)
- Citrate buffer for heat induced epitope retrieval (EMS 64142-08)
- Normal donkey serum (Jackson Immunoresearch 017-000-121)
- Whatman no. 1 filter for blocking solution (VWR 28450-150)
- Neurofilament H antibody (Sigma AB5539)
- Donkey anti-chicken IgY HRP-conjugated (Jackson Immunoresearch 703-035-155)
- ImmPact DAB substrate chromogen (Vector Labs SK-4105)
- 200 proof ethanol (VWR 89125-172)
- Xylene (Epredia 6601)
- Cytoseal 60 mounting medium (VWR 48212-154)
- 24x50 #1.5 coverslips (VWR 16004-322)

General Staining Notes

- Keep the hydrogen peroxide solution in the dark and do not use a solution older than 2 weeks.
- Do not use protein blocking solution older than 10 days. Always check to ensure the block is not cloudy and has no “floaters”. Filter before use.
- Avoid running water rinses where possible to minimize tissue disruption
- Ensure that all solutions are warmed to RT before applying to tissue.
- Vortex antibody stock briefly (2-3 seconds) then snap down or quickly centrifuge before diluting.

- Use time effectively to reduce length of procedure (e.g., make up diluted antibody during blocking step or washes, make up blocking solution during antigen retrieval step, use timer for each incubation, etc.).

Day 1 - deparaffinize and HIER start

Deparaffinization

1. Bake sections for 30 minutes at 55 C

2. Deparaffinize as follows:

a. 3x3 mins xylene

b. 2x1 min 100% OH

c. 1x1 min 95% OH

d. 30s 70% OH

e. DI water until HIER

Antigen retrieval (a.k.a. heat induced epitope retrieval, HIER)

1. Prepare citrate pH 6.0 antigen retrieval solution from 10X stock with DI water.

2. Place deparaffinized sections in the HIER solution at room temperature.

3. Transfer container to 55 C water bath for 18-20 hours (i.e. overnight).

Day 2 - Blocking, antibody incubations, chromogen development, counterstaining, mounting

4. The following morning, remove dish from water bath and allow to equilibrate at RT for 15-20 minutes.

5. Rinse with DI water 3 x 1 minute.

Peroxidase Block

1. Prepare 3% H2O2 solution in methanol by diluting 30% stock solution to volume (treat as 10X stock).

2. Briefly rinse slides in a dish of DI water, then transfer to peroxidase block for 10 minutes at room temperature (very important, make sure the solution is warmed to RT if reusing).

3. Rinse 3x1 min in DI water.

Permeabilization/Protein Block

1. Place 2-3 strips of absorbent cloth around tray. Add buffer solution to saturate and humidify staining chamber.

2. Dry off the back side of the slides, then place slides onto staining tray and flood slide with 0.5% TBS-Tween for 5 minutes. Do not let tissue dry completely at any point hereafter!

3. Tap off or aspirate excess solution, wipe carefully around tissue to dry, and apply a PAP pen barrier.

4. Apply a filtered solution of 5% normal donkey serum in 0.5% TBS-Tween for 30 mins to block non-specific binding.

Primary antibody incubation

1. Make up primary antibody working solution using stock antibody diluted in blocking solution. Assume 200 uL per slide and use a dilution of 1:1500 for NFH

2. Remove blocking solution from sections, then apply diluted antibody. Incubate for 1 hr at RT protected from light.

Secondary antibody Incubation

1. Rinse slides with 0.5% TBS-Tween 3 x 5 minutes.

2. Apply donkey anti-chicken HRP secondary diluted 1:250 in blocking solution for 1 hr at RT protected from light

HRP/DAB substrate reaction

1. Rinse slides 2 x 5 minutes with 0.5% TBS-Tween to remove secondary antibody. Transfer to TBS for 1 minute minimum (can hold here for up to an hour if needed)

2. Make up DAB solution using 1 drop concentrate to 1 mL of buffer

3. Just before adding chromogen, wash slides for 1 minute in DI water.

4. Add chromogen to slides and incubate for 2 minutes, then end reaction by placing slides in a dish of DI water. Rinse in DI water 3x1 minute

Counterstain

1. Dip the slides into Mayer's hematoxylin for 1 minute

2. Wash 4 x 30s in DI water

3. Transfer to 0.1% sodium carbonate for 1 minute to blue nuclei

Dehydration & Mounting

1. 70 OH 10 seconds

2. 95 OH 10 seconds

3. 100 OH 30 seconds x 3

4. XY 3 x 1 min

5. Coverslip with cytoseal or other xylene based medium

Appendix B

Illustration of Impact Loading System

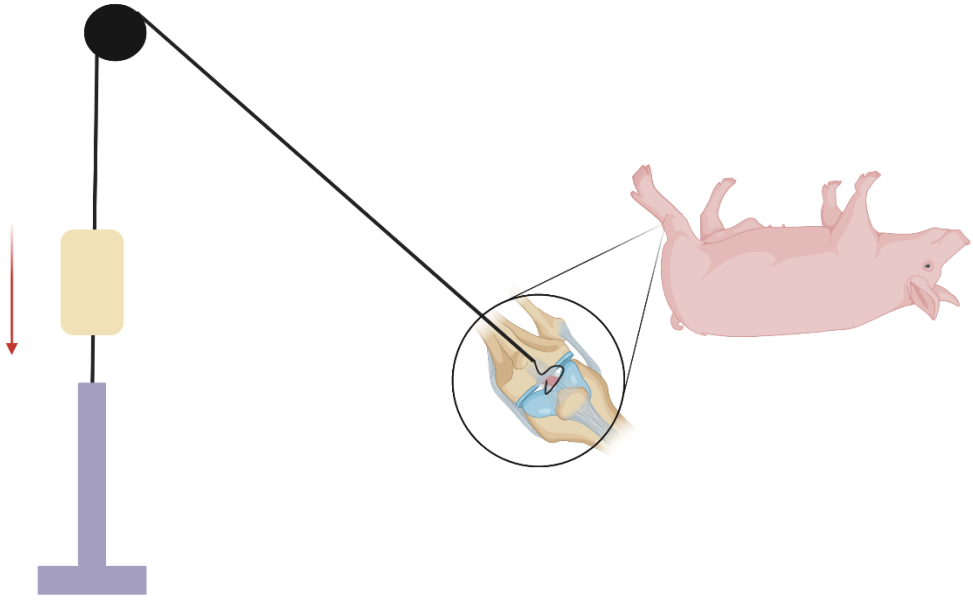

Appendix C

Atlas for Mechanoreceptor Identification

Morphology

- **Overall shape:** Mechanoreceptors typically present as circular, oval, elliptical, spindle-shaped, or elongated fusiform structures

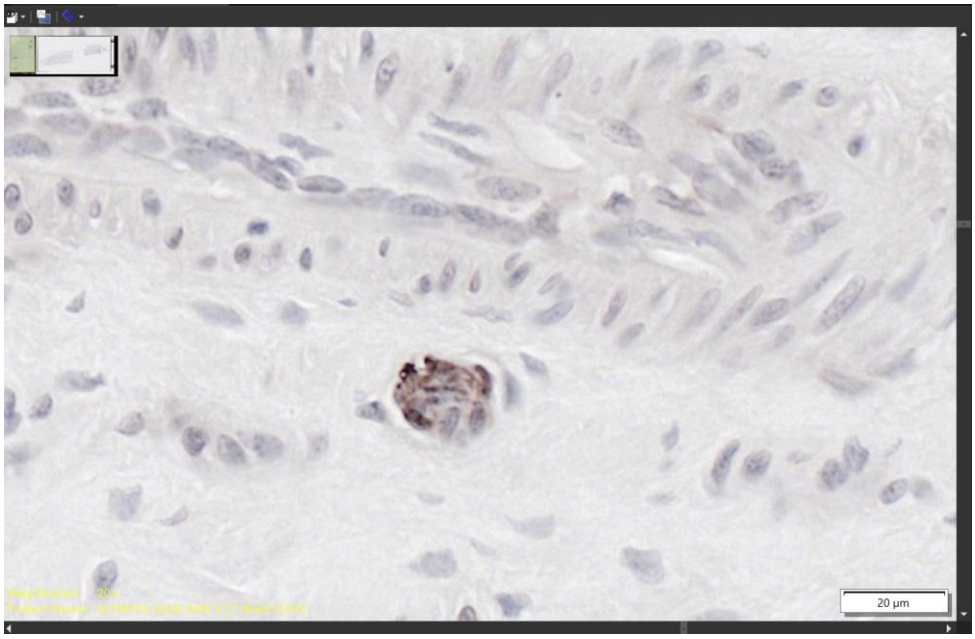

Slice 5

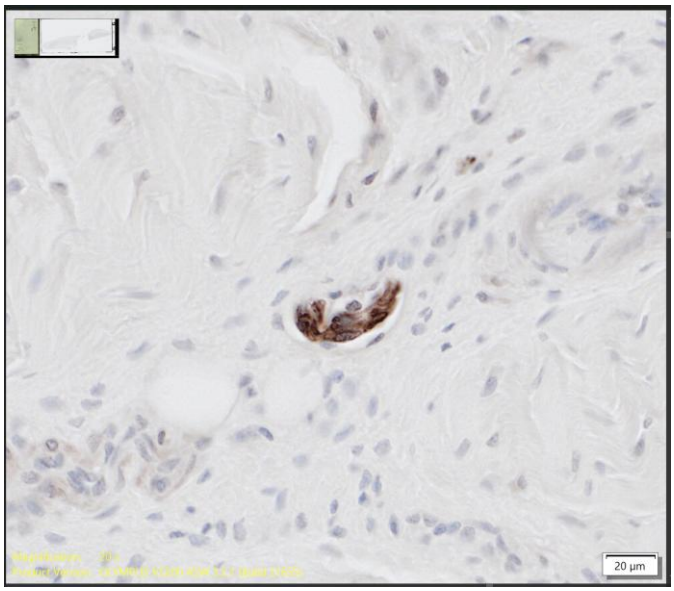

Slice 7

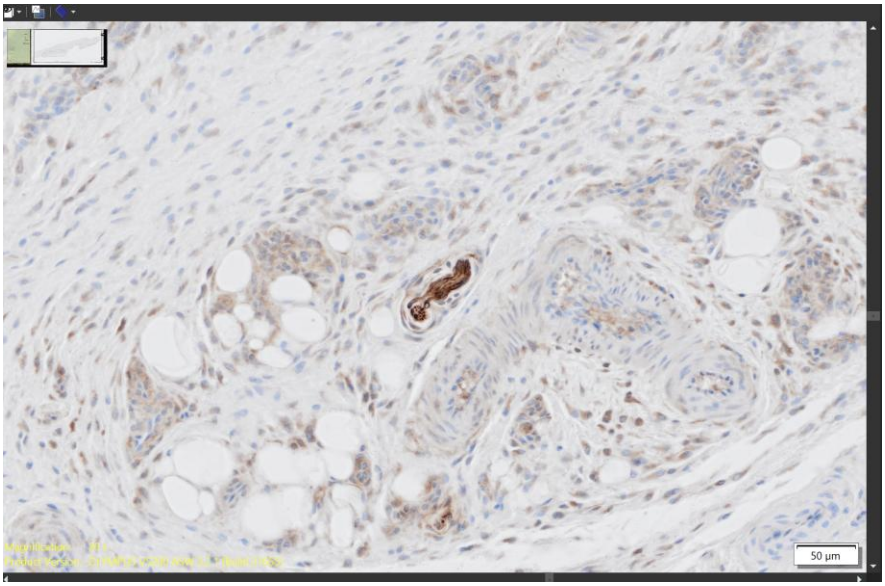

Slice 21

- **Membrane or layers:** Mechanoreceptors often exhibit a thin membrane or multiple layers of collagen fibers arranged concentrically, resembling "onion skin" architecture

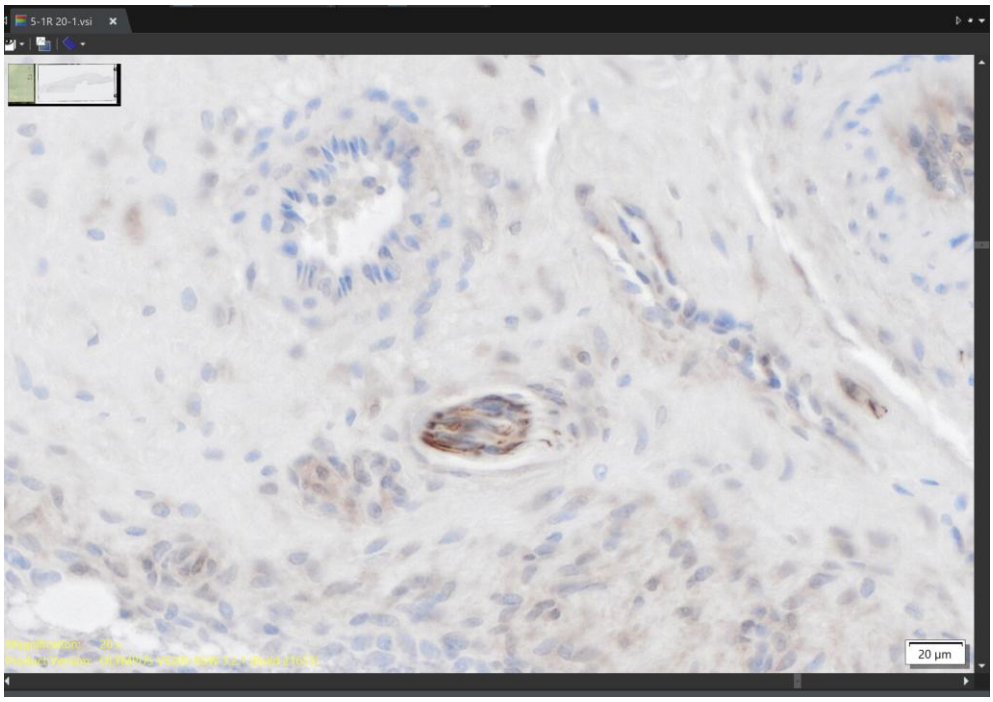

Slice 20

- **Size criteria:** There is considerable variability in the reported sizes of mechanoreceptors. Accepted dimensions from the literature include:
    - 50-200 µm diameter [67]
    - 50-500 µm , 100-600 µm [68]
    - 20-40 µm [69]
    - 2-6 cylinders in a ruffini corpuscle and each cylinder's diameter is 3-4 µm [69]
    - Additionally, Freeman and Wyke's classification specifies approximate dimensions [26]:
        - Ruffini endings: 100 × 40 µm
        - Pacinian corpuscles: 280 × 120 µm
        - Golgi tendon organs: 600 × 100 µm

Mechanoreceptors falling within the 20–600 µm range, and fulfilling the other criteria outlined here, were accepted.

Staining Intensity and Color

- **Accepted staining characteristics:** On a subjective scale of 1–10 (1 being very faint, 10 being very dark), acceptable mechanoreceptors ranged from approximately 3-4 to darker intensities for examiner 1. For example, one accepted mechanoreceptor exhibited lighter staining on the left side and darker staining on the right.

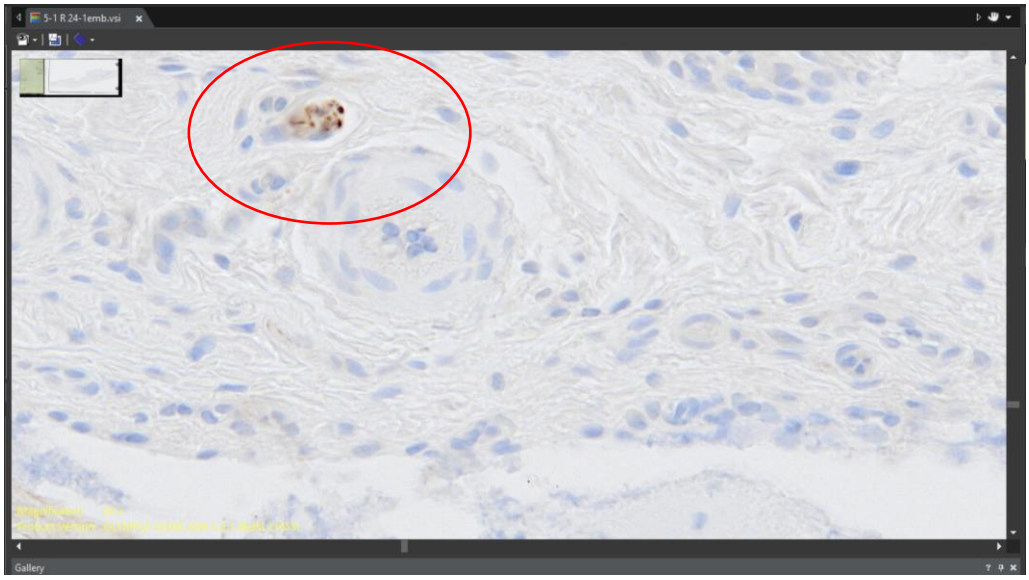

Slice 24: Rated 3-4/10 on the lighter ends of the mechanoreceptor

- **Rejected staining characteristics:** Structures exhibiting very faint staining (rated 1–3/10 by examiner 1) without clearly discernible morphology were not classified as mechanoreceptors.

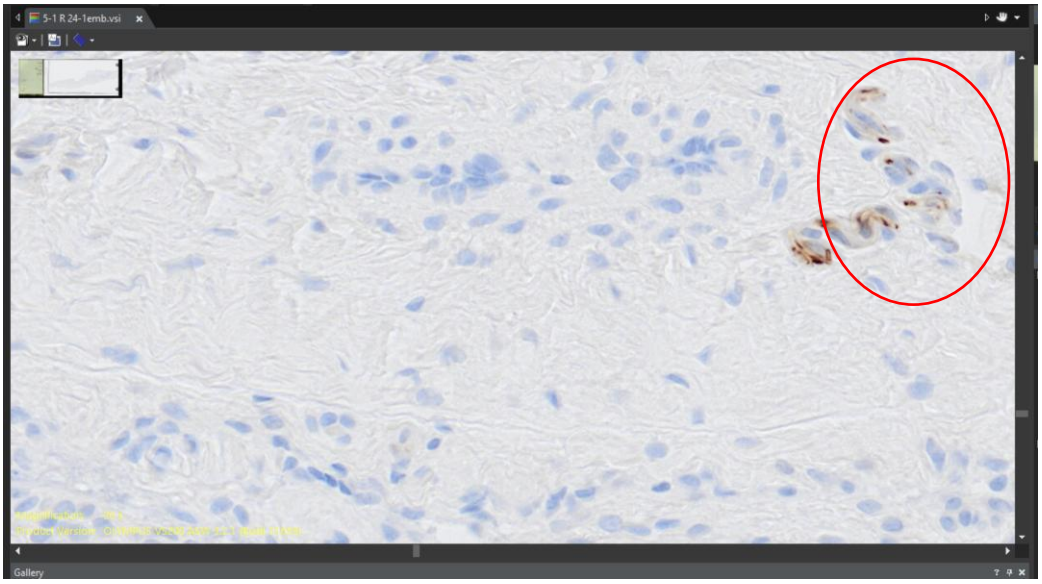

Slice 24: rated 1-2/10 on the lighten ends of the structure

Proximity to Blood Vessel

Mechanoreceptors may be located near blood vessels; however, clear distinction between neural structures and vasculature must be made.

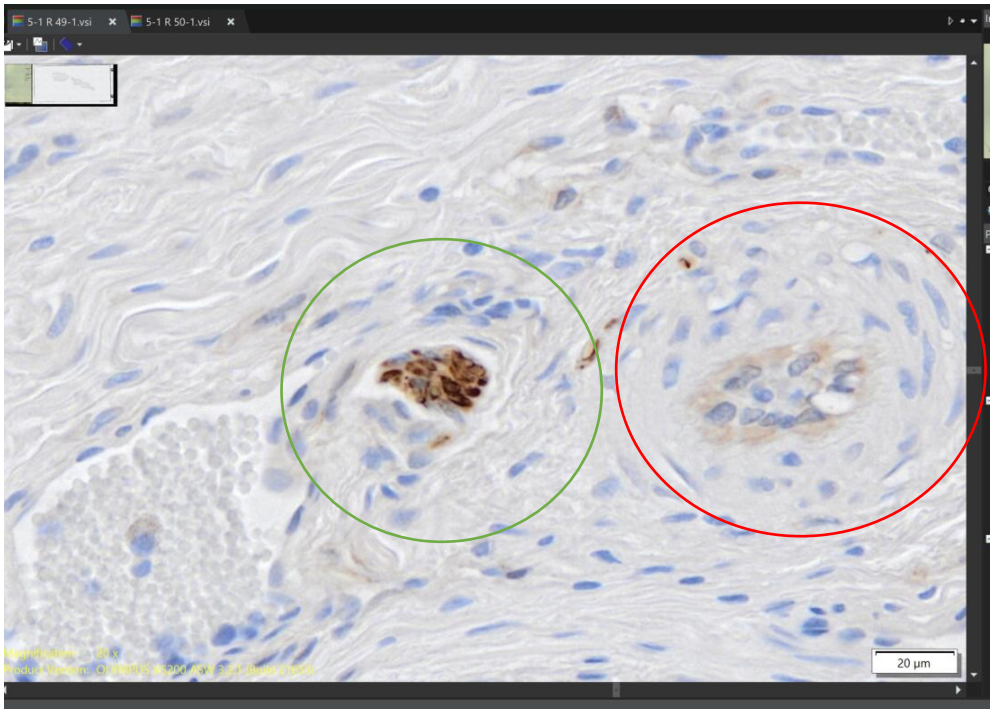

Slice 49: blood vessel marked in red, mechanoreceptor marked in green

Tissue location

Mechanoreceptors were only identified if located within ligamentous tissue. Structures found within bone and not the insertion sites or ligament were excluded.

Staining or Tissue quality

Sections where staining or tissue morphology appeared blurred or degraded were excluded from mechanoreceptor counting. Identification was only accepted when both staining and tissue quality allowed for confident classification.

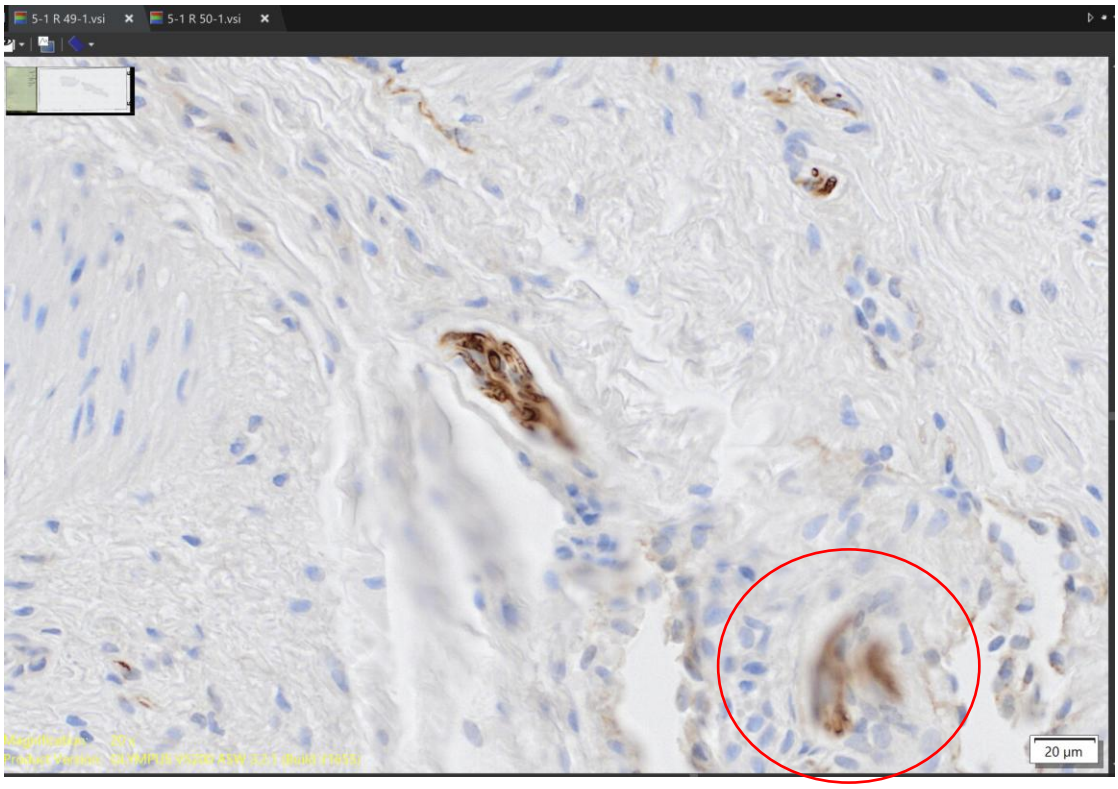

Slice 49: Rejected mechanoreceptor marked in red

Artifact Staining

- **Nerve fiber artifacts:** Long, linear structures with diffuse staining that did not fit the typical mechanoreceptor morphology were identified as nerve fibers rather than mechanoreceptors and were excluded.

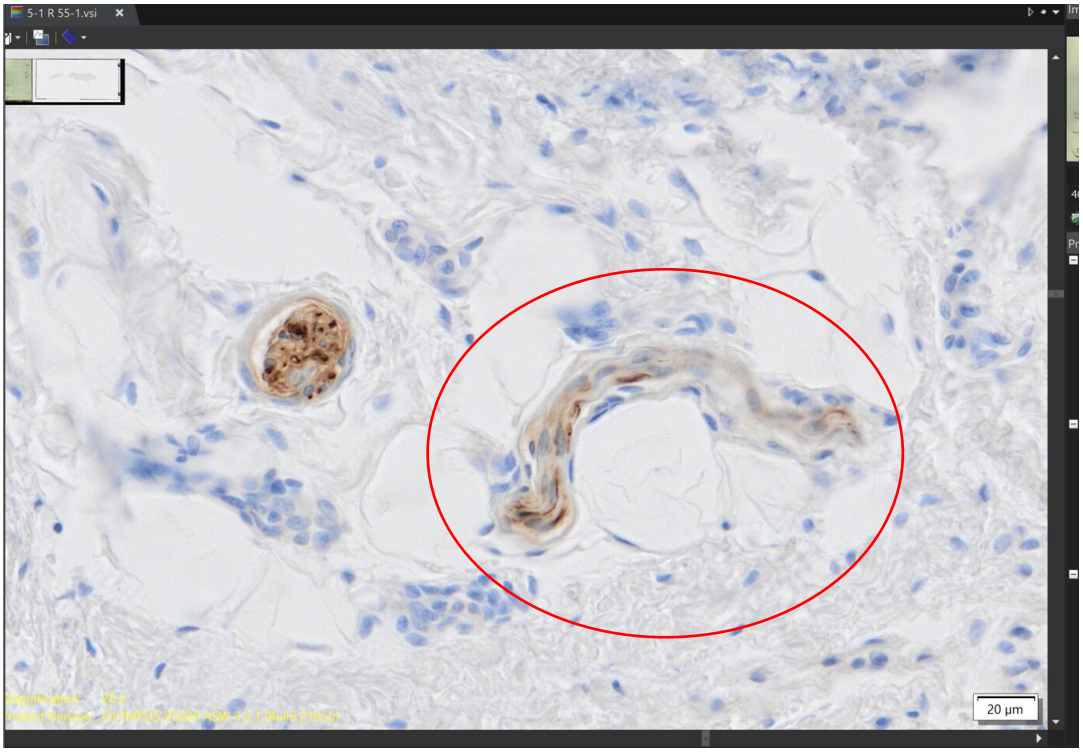

Slice 55: Stained structure marked in red

- **Blood vessel artifacts:** Structures presenting with a visible lumen or long linear structures were identified as blood vessels and excluded

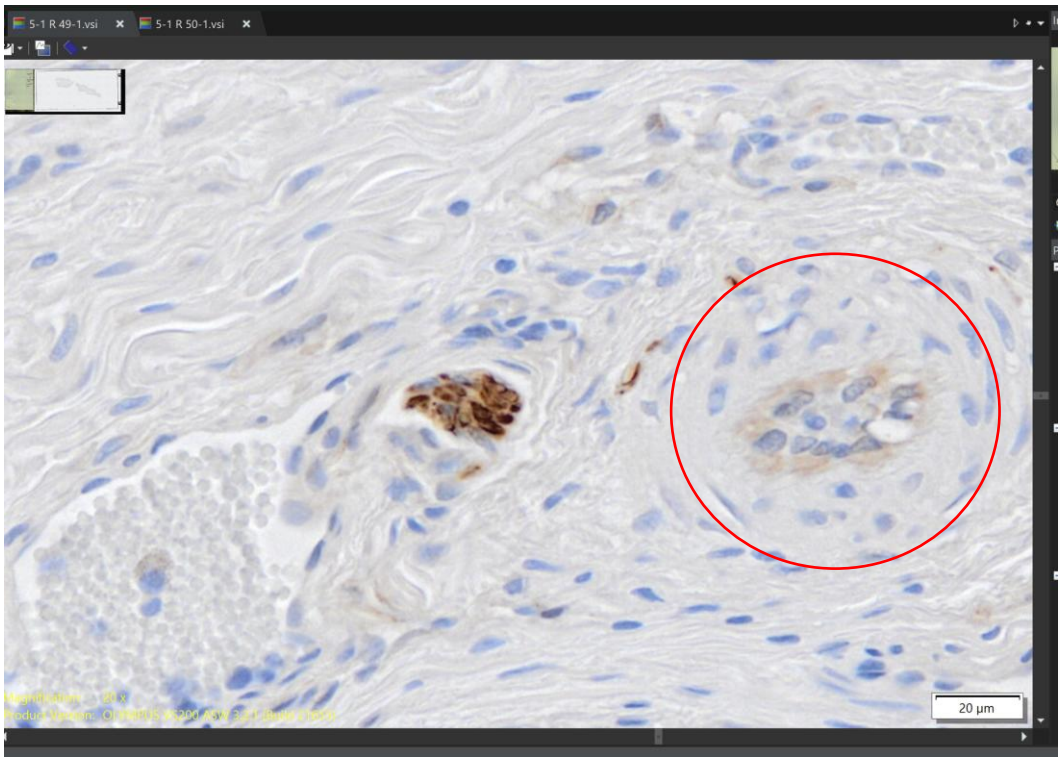

Slice 49: Lightly stained structure marked in red

Table: Summarized Mechanoreceptor Identification Table

Feature	Criteria for Acceptance
Overall Shape	Circular, oval, elliptical, spindle-shaped, or elongated (fusiform) morphology
Membrane or Layered Structures	Presence of thin membrane or multiple collagen layers ('onion-skin' pattern)
Size Range	Diameter between 20–600 µm (following literature ranges)
Staining Intensity	Moderate to dark staining (approximately 3-4/10 or higher)
Proximity to Blood Vessels	Mechanoreceptors near vessels accepted if clearly distinct from blood vessels

Tissue Location	Located within ligament tissue or insertion sites, not bone or degraded areas
Tissue Quality	Clear tissue structure and morphology; poor quality sections excluded
Artifact Types	Exclude structures with diffuse linear staining (nerve fibers) or lumen (blood vessels)

Summary

Mechanoreceptors were accepted for quantification based on a combination of morphology, size range, staining intensity, proximity to blood vessels, tissue location, and tissue quality. Structures that failed to meet these combined criteria were systematically excluded.